

Original Article

Molecular signature and pathway analysis of human primary squamous and adenocarcinoma lung cancers

Nikolai Daraselia¹, Yipeng Wang², Adam Budoff², Alexander Lituev³, Olga Potapova³, Gordon Vansant², Joseph Monforte², Ilya Mazo¹, and Valeria S Ossovskaya⁴

¹Ariadne Inc., Rockville, MD, USA; ²AltheaDx, San Diego, CA, USA; ³Cureline Inc., South San Francisco, CA, USA;

⁴BiPar Sciences, Inc. (subsidiary of Sanofi), South San Francisco, CA, USA

Received September 29, 2011; accepted October 22, 2011; Epub November 19, 2011; Published January 1, 2012

Abstract: Non-small cell lung cancer (NSCLC) is the most common type of lung cancer, with a poor response to chemotherapy and low survival rate. This unfavorable treatment response is likely to derive from both late diagnosis and from complex, incompletely understood biology, and heterogeneity among NSCLC subtypes. To define the relative contributions of major cellular pathways to the biogenesis of NSCLC and highlight major differences between NSCLC subtypes, we studied the molecular signatures of lung adenocarcinoma (ADC) and squamous cell carcinoma (SCC), based on analysis of gene expression and comparison of tumor samples with normal lung tissue. Our results suggest the existence of specific molecular networks and subtype-specific differences between lung ADC and SCC subtypes, mostly found in cell cycle, DNA repair, and metabolic pathways. However, we also observed similarities across major gene interaction networks and pathways in ADC and SCC. These data provide a new insight into the biology of ADC and SCC and can be used to explore novel therapeutic interventions in lung cancer chemoprevention and treatment.

Keywords: NSCLC, adenocarcinoma, squamous cell carcinoma, molecular signature, gene expression, pathway

Introduction

Worldwide, over 1.3 million people are diagnosed each year with lung cancer, with over 1.1 million deaths [1, 2]. Lung cancer is the most common global cause of cancer death in men and second only to breast cancer in women (17.6% of cancer-related deaths in both sexes) [1-3]. There is a high fatality rate with this disease, with only 15% of patients still alive 5 years after diagnosis [4]. Non-small cell lung cancer (NSCLC) is the most common type of lung cancer, accounting for 85% of cases, and can be divided into three main subgroups: adenocarcinoma (ADC; 30-50% of cases), squamous cell carcinoma (SCC; ~30%), and large cell carcinoma (LCC; ~10%), according to the predominant morphology of the tumor cells as determined by light microscopy [4-7]. NSCLC is associated with high rates of proliferation and metastases, as well as poor prognosis for advanced-stage disease compared with other cancers. There are several potential explanations for the disparity between lung cancer survival and other common tumors, including late detection and histologic heterogeneity. This heterogeneity is reflected by the fact that the majority of prostate, breast, and colorectal carcinomas are ADC, while only 30% of NSCLC cases are of this subtype [6, 8]. For the most part, and until recently, NSCLC subtypes (SCC, LCC, and ADC) were treated similarly, regardless of the biologic heterogeneity associated with histology. It is likely that poor historic lung cancer response rates may be attributable in part to a relatively homogenous approach to treat a heterogeneous disease. Therefore, a better understanding and molecular characterization of the NSCLC subtypes could contribute to improved design of treatment schedules and management of lung cancer.

Gene expression profiling using microarrays is a robust and straightforward way to study the molecular features of different types and subtypes of cancer at a systems level. Although it is possible to distinguish the different NSCLC subgroups histologically, genomic profiling demonstrates that there are significant and distinct differences in the molecular signature associated with each subtype [9-12]. In addition, gene expression profiles have been used to predict patient survival and response to therapy [13-16].

Recently, we performed a genome-wide gene expression analysis of lung ADC and SCC samples and found significant differences in gene expression profiles between these two subtypes [17]. We also found that ADC and SCC share many common gene expression patterns, particularly in the cell cycle, DNA repair, and metabolic pathways. These findings support the notion that ADC and SCC are biologically similar and may benefit from similar therapeutic interventions. In this study, we analyzed the molecular signatures of lung ADC and SCC, based on gene expression analysis and comparison of tumor samples with normal lung tissue. Our results suggest the existence of specific molecular networks and subtype-specific differences between lung ADC and SCC subtypes, mostly found in cell cycle, DNA repair, and metabolic pathways. However, we also observed similarities across major gene interaction networks and pathways in ADC and SCC. These data provide a new insight into the biology of ADC and SCC and can be used to explore novel therapeutic interventions in lung cancer chemoprevention and treatment.

ated with each subtype. The objective of this study was to enhance the understanding of NSCLC pathogenesis through characterization of molecular and pathway signatures in primary lung ADC and SCC samples, and to compare these signatures with those of normal lung tissue.

Materials and methods

Isolation of RNA

Sets of syngeneic normal and tumor samples (lung ADC and SCC) were obtained from Cureline Biobank (Cureline Inc., San Francisco, CA). Eighty formalin-fixed, paraffin-embedded (FFPE) tissue samples from 20 patients with NSCLC were analyzed (20 FFPE tissue samples for each group). For RNA isolation, five 10- μ m sections were sliced via microtome, placed in 1.7 ml tubes, and deparaffinized with 1 ml of xylene (EMD Chemicals, Gibbstown, NJ). The samples were digested for 16 hours with Proteinase K and total RNA isolation was performed using the Epicentre Biotechnologies MasterPure™ Complete DNA and RNA Purification Kit (Epicentre Biotechnologies, Madison, WI) following the manufacturer's instructions. All samples were subsequently treated with RNase-free DNase I (Ambion, Austin, TX).

Synthesis of cDNA, amplification, and labeling

RNA samples were amplified and converted to cDNA using the NuGEN WT-Ovation FFPE v2 RNA Amplification System (NuGEN Technologies, San Carlos, CA) [9, 10]. Briefly, 50 ng of RNA was reverse transcribed to antisense-cDNA, amplified using kit reagents, and purified using a QIAGEN PCR purification kit (QIAGEN, Valencia, CA). DNA concentration was assessed using a Nanodrop ND-100 spectrophotometer. Sense transcript cDNA (ST-cDNA) was generated from 2-4 μ g of purified antisense-cDNA using the kit reagents according to manufacturer's instructions. ST-cDNA was purified by QIAGEN kit and final DNA concentration determined by absorption. Up to 5 μ g of purified ST-cDNA was fragmented and biotin-labeled using the NuGEN Encore Biotin Module Kit (NuGEN Technologies, San Carlos, CA).

Hybridization, washing, and analysis

Biotin-labeled cDNA from each sample was directly hybridized to GeneChip Human Gene 1.0

ST Arrays (Affymetrix, Santa Clara, CA) along with GeneChip Eukaryotic Hybridization controls (Affymetrix, Santa Clara, CA). Samples were incubated at 45°C in an Affymetrix hybridization oven 640 at 60 rpm for 16 hours, and washed with an Affymetrix GeneChip Fluidics Station 450 according to the manufacturer's specifications. Scanning was performed using the Affymetrix GeneChip 7G scanner using manufacturer-recommended default settings.

Data analysis

An Affymetrix Expression Console was used to generate quality control parameters, process probe intensity files and CEL-format data files, and to normalize and summarize a gene expression measurement for each probe set on the array through a Robust Multiarray Averaging (RMA) algorithm [11]. All the clinical and control samples in the study and the expression values were log-transformed with a base of 2 for downstream data analysis. For each individual sample, differential expression profiles of cancer versus normal syngeneic tissue were calculated. In addition, differential profiles of all cancer samples versus all normal breast samples were calculated using an unpaired t-test.

All gene expression analyses were performed in Pathway Studio 7 (Ariadne Genomics, Inc., Rockville, MD) [9, 11-15], using the ResNet 7 database (Ariadne Genomics, Inc.) [9, 10]. Enrichment analysis in Pathway Studio 7 was performed by Gene Set Enrichment Analysis (GSEA) [16] and Sub-Network Enrichment Analysis (SNEA) algorithms ([Supplementary Figure 1S](#)) [11]. Functional enrichment was performed using Fisher's Exact Test.

SNEA enrichment in Pathway Studio was calculated using the Mann-Whitney test, a non-parametric method that compares the medians of non-normal distributions X and Y. Both samples (having sizes N and M) are combined into one array in ascending order with each element then replaced by its rank in the array from 1 to N+M. The ranks of the first sample elements are summarized and a Mann-Whitney U-value calculated from **Equation 1**:

$$U = NM + \frac{N(N+1)}{2} - \sum_{x_i} Rank(x_i) \quad \text{Eq. 1}$$

If U is close to the mean of U (i.e. $0.5 \cdot N \cdot M$) then the medians of X and Y are similar. The significance level of the U statistic can be derived from the distribution quantiles. When applied to gene expression data, two distributions are typically derived from the gene set or sub-network, and from the entire gene expression profile measured on the chip. The following steps describe the computational steps performed by the SNEA algorithm.

Preparation of sub-networks

SNEA was used to build sub-networks from the relationships in a database based on criteria specified by the user. A central 'seed' is initially created from all relevant entities in the database, and associated entities retrieved based on their relationship with the seed (binding partners, expression targets, protein modification targets, etc.).

Calculation of background distribution

This algorithm was used to calculate a background distribution of all expression values for the selected sample in the experiment, typically from a differential measurement such as that resulting from the 'Find Differentially Expressed Genes' tool.

Calculation of sub-network distribution

This algorithm was used to create a 'sub-network' distribution of the expression values in a similar manner for all sub-networks constructed in the previous step. More importantly, during distribution calculation, the expression value for each entity connected to a seed is accounted for as many times as the connectivity of that entity in ResNet. The purpose of this correction is to correct the bias introduced by the different connectivity of entities in ResNet.

Statistical comparison of sub-network distribution with background distribution

This algorithm is used to compare the sub-network distribution with the background distribution using a one-sided Mann-Whitney U -test, and calculates a p-value indicating the statistical significance of difference between two distributions. Presentation and prioritization of results were done with Pathway Studio, which presents the 'seed' entity for each sub-network

along with the sub-networks themselves in the user interface, ranked from the lowest (best) to the highest (worst) p-value. Note: the percentage overlap is also presented in order to provide an adequate measurement of significance and confidence in various statistical tests of overlap.

Analysis of key regulators of differential gene expression

The key regulators of differential response are those components of signal transduction pathways and expression regulators that are most likely to be involved in the regulation of genes differentially expressed between tumor and normal samples. Such key regulatory signaling pathways are assumed to be deregulated (e.g. abnormally activated or suppressed) in a disease state and provide insights into the mechanisms and molecular features of a disease. Our analysis implements a proprietary SNEA algorithm, which utilizes a gene expression regulatory network built from facts extracted from the literature. The network is used to generate a comprehensive collection of gene sets, each representing immediate downstream neighbors of each individual protein in the network. It is assumed that if the downstream expression targets of the central seed protein are enriched with differentially expressed genes (i.e. the sub-network is found to be statistically significant in enrichment analysis), then the seed protein is one of the key regulators of the observed differential response. As sub-networks are constructed from all the proteins in the entire expression network, including ligands, receptors, signaling proteins, and transcription factors, the seed proteins of statistically significant sub-networks presumably constitute the components of a regulatory network involved in the modulation of the observed differential response.

Results

Significant regulators of ADC and SCC

We focused our analysis on the regulation of major cellular pathways. The key regulators of differential response were identified by searching for all expression sub-networks in the ResNet 7 database enriched with differentially changed genes using a Mann-Whitney test with a p-value cut-off of 0.001. We performed analyses separately for lung SCC and ADC, and all

Table 1. Significant regulators in lung adenocarcinoma (ADC) and squamous cell carcinoma (SCC) by SNEA (Mann-Whitney p<0.001)

Name	Sub-network size	Median fold change	p-value
Adenocarcinoma			
CTGF	47	1.02072	8.98 × 10 ⁻⁵
S100A4	15	1.28985	1.52 × 10 ⁻⁴
Vitronectin receptor	21	1.14296	2.38 × 10 ⁻⁴
E2F3	34	1.20872	3.45 × 10 ⁻⁴
PDGF	285	1.01231	4.48 × 10 ⁻⁴
miR-200	5	-1.52286	4.74 × 10 ⁻⁴
E2F4	40	1.18259	8.11 × 10 ⁻⁴
EMP2	5	-1.48652	8.50 × 10 ⁻⁴
RB1	75	1.10424	8.61 × 10 ⁻⁴
Squamous cell carcinoma			
PDGF	285	-1.03133	3.05 X 10 ⁻⁵
EGF	393	-1.01802	3.33 X 10 ⁻⁵
CTGF	47	-1.03683	2.61 × 10 ⁻⁴
CX3CL1	11	-1.45216	4.38 × 10 ⁻⁴
E2F4	40	1.3792	4.98 × 10 ⁻⁴
IL1F8	34	-1.11308	5.47 × 10 ⁻⁴
E2F3	34	1.3792	8.09 × 10 ⁻⁴
PRKCB	33	-1.17599	8.97 × 10 ⁻⁴
COMP	9	-1.45216	9.25 × 10 ⁻⁴

identified significant regulators are shown in **Table 1**. We found that transcription factors associated with differential expression in both ADC and SCC, in comparison with normal lung tissue, were representatives of the E2F family (E2F3 and E2F4). The connective tissue growth factor (CTGF) and platelet-derived growth factor (PDGF) pathways are also significantly changed in both subtypes of NSCLC. The retinoblastoma (Rb1) pathway is up-regulated specifically in ADC, whereas the epidermal growth factor (EGF) pathway is significantly affected (down-regulated) only in SCC. Lung ADC samples show significant and specific down-regulation of the miR-200 molecular network and the epithelial membrane protein 2 (EMP2). The miR-200 family of microRNAs plays a major role in specifying the epithelial phenotype by preventing expression of the transcription repressors ZEB1/deltaEF1 and SIP1/ZEB2, and regulates epithelial-mesenchymal transition [17]. EMP2 controls surface levels of several classes of integrin and other cell-interaction molecules, and their trafficking to glycolipid-enriched lipid raft domains is important in receptor signaling [18]. Lung SCC samples show down-regulation of chemokine (C-X3-C motif) ligand 1 (CX3CL1),

interleukin-1 family member 8 (IL1F8), and protein kinase C beta (PRKCB) pathways.

DNA repair, cell proliferation, and apoptotic pathways

DNA damage repair is a complex and multifaceted process that is critical to cancer cell survival and response to DNA-damaging chemotherapy. To define the relative contributions of DNA repair to ADC and SCC, we investigated the differential changes in all known DNA repair pathways. The record of genes and proteins involved in the regulation of DNA repair pathways were assembled using the ResNet 7 database and then verified as described previously [19]. **Figures 1, 2, and 3** show graphically the changes in differential gene expression between all lung cancer samples and normal tissue among DNA-repair pathways, cell-cycle pathways, and apoptosis pathways, respectively, and defined by differential changes of the pathway proteins. Individual gene expression differences and p-values for components of each of these pathway types are provided in Supplementary **Tables S1, S2, and S3**, respectively.

Molecular signature of lung cancers

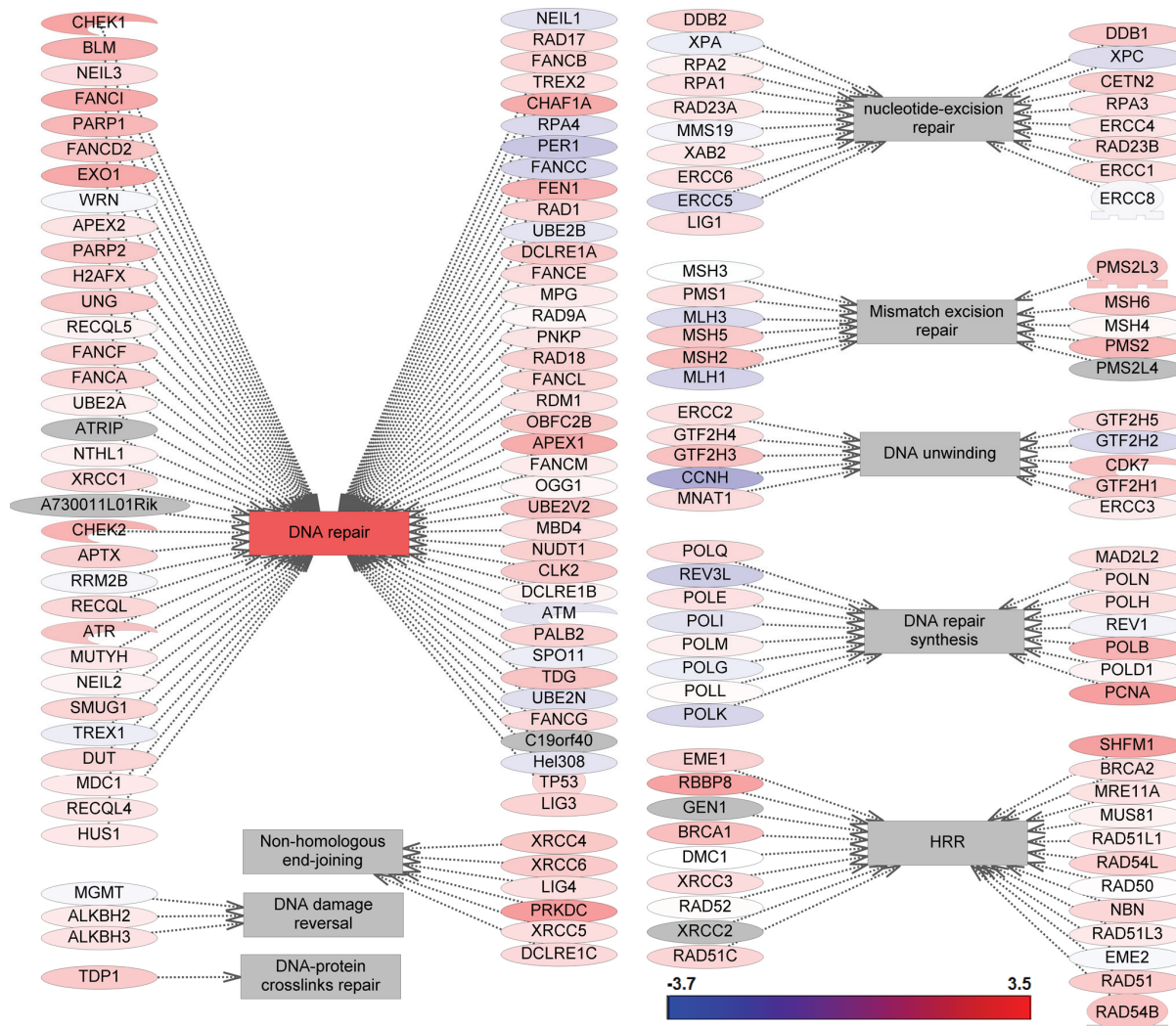


Figure 1. Gene expression changes in DNA repair pathways.

DNA repair components significantly up-regulated (2-fold or more with $p < 0.001$) in lung SCC included retinoblastoma-binding protein 8 (RBBP8), protein kinase DNA-activated catalytic polypeptide (PRKDC), split hand/foot malformation (ectrodactyly) Type 1 (SHFM1), and proliferating cell nuclear antigen (PCNA). By contrast, there were no significant changes in expression of DNA-repair genes in lung ADC.

Cell-cycle genes were more significantly up-regulated in SCC than in ADC. Topoisomerase (DNA) II alpha (170 kD) (TOP2A), cyclin B1 (CCNB1), maternal embryonic leucine-zipper kinase (MELK), mitotic arrest deficient-like 2 (yeast), human homolog like-1 (MAD2L1), strati-

fin (SFN), cell division cycle 6 homolog (CDC6), abnormal spindle-like microcephaly-associated protein (ASPM), and DNA topoisomerase binding protein 1 (TOPBP1) were all significantly up-regulated in SCC. By contrast, only TOP2A was significantly up-regulated in ADC.

Among apoptotic pathways, CASP8 and FADD-like apoptosis regulator (CFLAR) was significantly down-regulated (-2.34) in SCC. No other apoptotic proteins were significantly changed in any of the ADC or SCC samples.

The SNEA approach was also applied to identify key regulators and detect global cell proliferation processes significantly affected in NSCLC.

Molecular signature of lung cancers

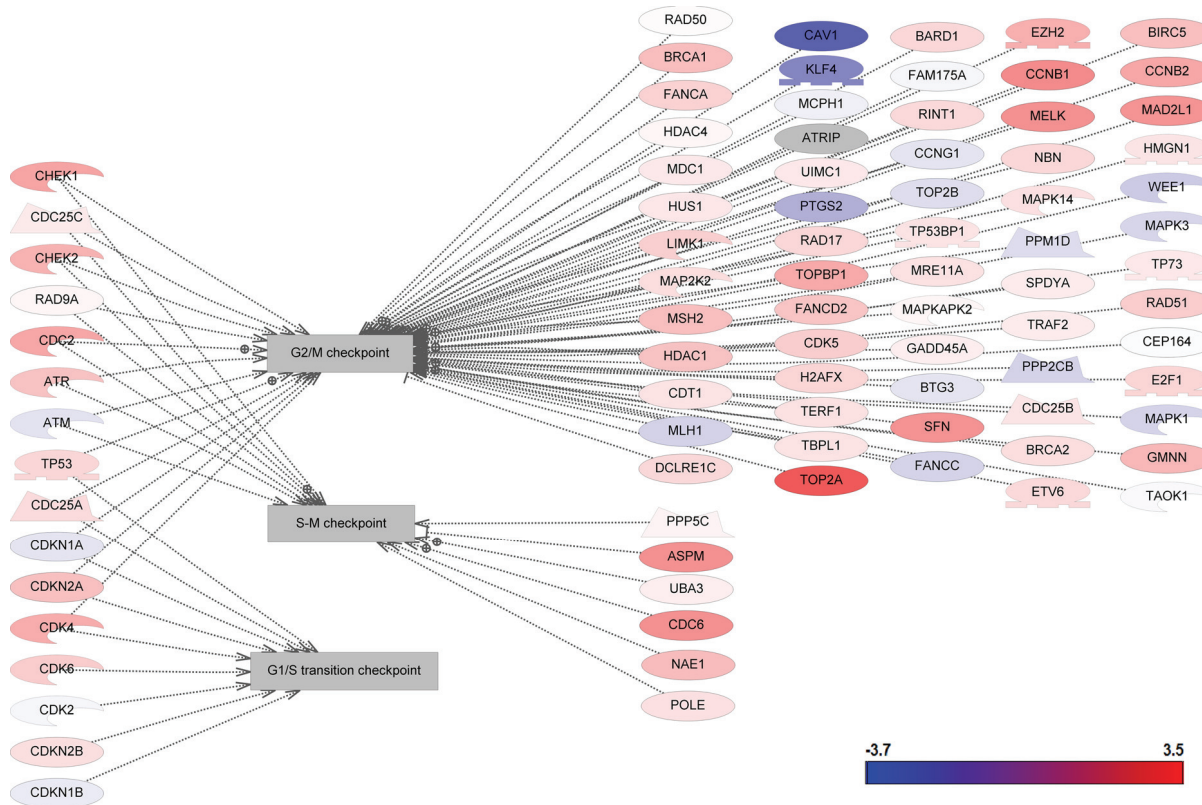


Figure 2. Gene expression changes in cell cycle pathways.

In this approach, sub-networks were built around each cell process in the ResNet 7 database and contained all proteins known to be involved in the regulation of the process (SNEA was applied with a Mann-Whitney p-value cut-off value of 0.001). Significantly affected processes are documented in **Table 2**. Most of the significantly affected processes in both lung cancer subtypes are related to cellular proliferation (spindle assembly, chromosome segregation, cytokinesis, kinetochore assembly, mitotic checkpoint, etc.), as would be expected in actively proliferating lung tumor cells. Other cellular processes are related to metastasis, including extracellular matrix remodeling, cell invasion, and cell-cell contact. In general, changes were similar across subtypes.

Metabolic pathways

Because the cell cycle is functionally linked to cellular metabolism and energy production, we next analyzed the differential gene expression of ADC and SCC versus pathologically normal lung tissue and all metabolic pathways in the

ResNet 7 database, using the GSEA algorithm, and a Mann-Whitney test with p-value cut-off at 0.05. Significantly changed metabolic processes for each lung cancer subtype are documented in **Table 3**. Purine and pyrimidine synthesis pathways were significantly up-regulated in both subtypes. The SCC type also demonstrated up-regulated energy production pathways for oxidative phosphorylation, glucose metabolism, and the tricarboxylic acid cycle. These findings are consistent with active DNA synthesis and active proliferation of lung cancer cells.

Oncogenes and tumor suppressors

Because oncogenes and tumor suppressors play a significant role in the regulation of cell proliferation, we next investigated a major molecular network of 273 oncogenes and 92 tumor suppressors in ADC and SCC using the ResNet 7 database. The oncogenes with at least 2-fold change ($p < 0.001$) are documented in **Table 4**. All oncogenes in ADC, and most in SCC, with the exception of ECT2 (elevated 3.6-fold) and DCUN1D1 (elevated 2.7-fold), were significantly

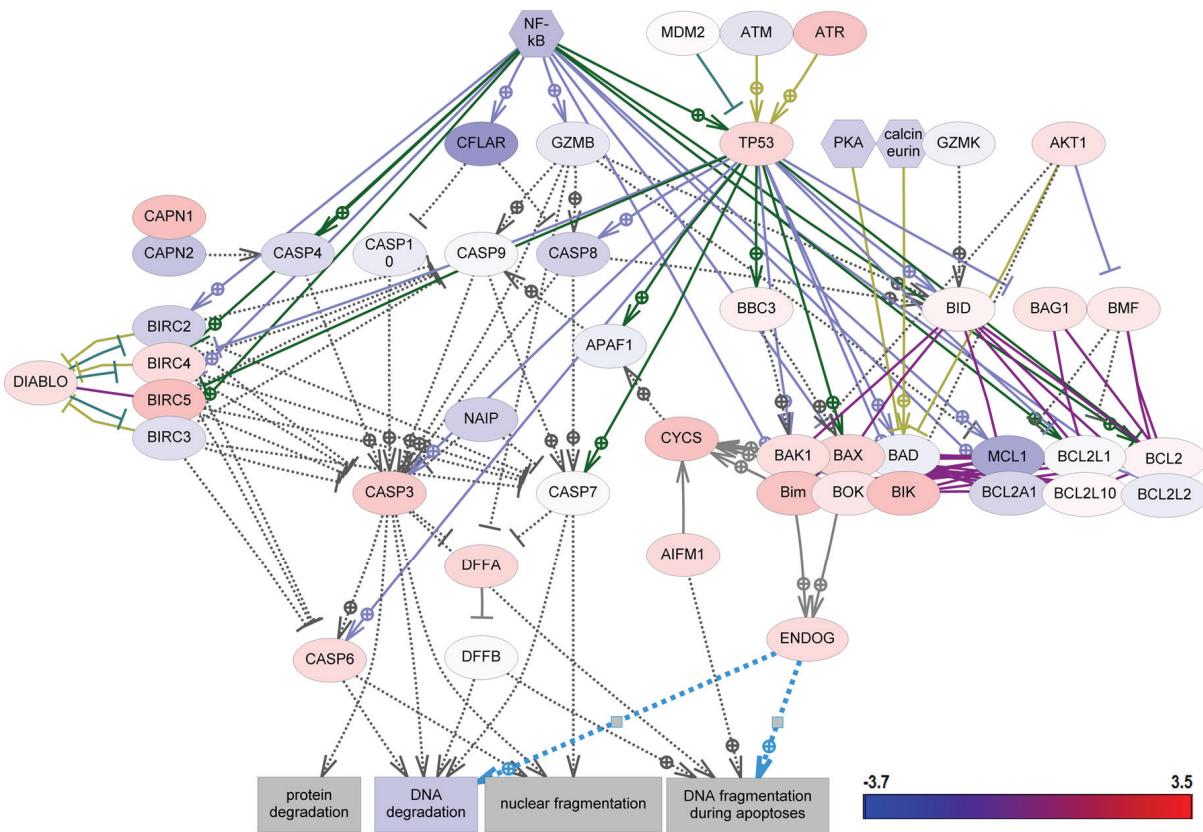


Figure 3. Gene expression changes in apoptotic pathways.

down-regulated. The oncogenes down-regulated in both types of lung cancer included FOS and FOSB. Changes in tumor suppressors were examined (**Table 4**) for both lung cancer subtypes. Tumor suppressors were not changed significantly in ADC, whereas in SCC, DLG1 and DLGAP5 were up-regulated, and TGFBR2 was down-regulated. Full details of differential changes in oncogenes and tumor suppressors (including p-values) are provided in Supplementary **Tables S4** and **S5**, respectively.

Discussion

NSCLC represents a heterogeneous collection of cancer subtypes that arise as a consequence of altered gene expression and mutations acquired during cancerogenesis. Molecular signatures of NSCLC subtypes can underline mechanisms of this complex disease and more importantly can facilitate the development of novel targeted therapy for cancer patients. Here we reported major cellular pathways of human lung ADC and SCC and described similarities as well

as unique differences between these two subtypes of lung cancer.

Sub-Network Enrichment Analysis (SNEA)

To build comprehensive molecular signatures of ADC and SCC, we used the SNEA algorithm, which is designed to investigate variations in gene set enrichment. Unlike previously reported approaches, such as GSEA, which uses a predefined collection of hand-curated gene sets [16], SNEA uses the global literature-extracted gene-gene expression regulation network to generate a comprehensive collection of gene sets [11]. The global expression network used for SNEA in this study is extracted and comprised over 160,000 independently reported relations [11]. The advantage of the SNEA application for this type of analysis is in the unbiased knowledge-driven nature of this approach. Sub-networks in SNEA are calculated from gene expression regulation ‘facts’ extracted across the entire PubMed database. Thus, each individual relation can come from specific and perhaps very nar-

Molecular signature of lung cancers

Table 2. Cellular processes significantly changed in lung adenocarcinoma (ADC) and squamous cell carcinoma (SCC) by SNEA (Mann-Whitney p<0.001)

Cellular process	Sub-network size	Median fold change	p-value
Adenocarcinoma			
Wound healing	385	1.02072	2.19×10^{-6}
ECM proteins	571	1.0277	2.38×10^{-6}
Chromosome segregation	149	1.10384	7.32×10^{-6}
Tissue remodeling	168	1.05076	1.16×10^{-5}
Cell survival	1251	1.03351	6.44×10^{-5}
Cell invasion	486	1.02405	7.79×10^{-5}
Tissue invasion	40	1.11402	1.23×10^{-4}
Mitotic cell cycle	37	1.10189	2.31×10^{-4}
G2/M transition	465	1.05898	2.37×10^{-4}
Abscission	25	1.00683	2.82×10^{-4}
Oncogenesis	347	1.02691	4.62×10^{-4}
Mitotic entry	123	1.07766	4.95×10^{-4}
Centrosome separation	38	1.13508	5.83×10^{-4}
Drug resistance	244	1.04375	7.66×10^{-4}
Cell redox homeostasis	18	1.12308	7.79×10^{-4}
Cell motility	691	1.02671	7.94×10^{-4}
Mitotic checkpoint	57	1.11636	8.92×10^{-4}
Cell contact	929	1.02568	9.04×10^{-4}
Squamous cell carcinoma			
Chromosome segregation	149	1.1897	4.58×10^{-10}
Kinetochore assembly	126	1.23986	7.28×10^{-10}
Mitosis	924	1.05925	1.35×10^{-8}
Spindle assembly	386	1.08566	6.70×10^{-8}
Cytokinesis	291	1.05385	1.03×10^{-7}
ECM proteins	571	-1.02692	2.90×10^{-7}
Wound healing	385	-1.05074	2.44×10^{-6}
DNA replication initiation	41	1.3792	1.02×10^{-5}
Mitotic checkpoint	57	1.24069	1.03×10^{-5}
Cell invasion	486	-1.01081	1.20×10^{-5}
Mitotic spindle assembly	41	1.23754	2.72×10^{-5}
G2/M transition	465	1.05662	2.81×10^{-5}
Premeiotic DNA synthesis	17	1.44176	3.11×10^{-5}
Cell motility	691	-1.01698	3.41×10^{-5}
Mitotic entry	123	1.1247	3.64×10^{-5}
Drug resistance	244	1.01383	4.29×10^{-5}
DNA replication checkpoint	40	1.35065	5.73×10^{-5}
Genome instability	178	1.13299	7.80×10^{-5}
S phase	737	1.02773	2.19×10^{-4}
DNA unwinding	117	1.15665	2.39×10^{-4}
Tissue remodeling	168	-1.03451	3.11×10^{-4}
Chromosome condensation	174	1.05662	3.14×10^{-4}
Cell growth	2072	1.00691	3.18×10^{-4}
Centrosome separation	38	1.30654	4.21×10^{-4}
Translation	689	-1.01232	4.53×10^{-4}
Cell division	598	1.00883	4.69×10^{-4}
Chemosensitivity	129	1.03154	4.94×10^{-4}
Cell-cell contact	307	-1.04502	5.89×10^{-4}
rRNA processing	69	1.21023	6.52×10^{-4}

Molecular signature of lung cancers

Table 3. Metabolic pathways significantly changed in lung adenocarcinoma (ADC) and squamous cell carcinoma (SCC) by GSEA (Mann-Whitney test, p<0.05)

Name	Sub-network size	Median fold change	p-value
Adenocarcinoma			
Nicotinate and nicotinamide metabolism	79	1.05861	2.953×10^{-3}
Glut/Gln/Pro metabolism	38	1.11358	1.0798×10^{-2}
Bile acids metabolism	41	1.04722	1.1389×10^{-2}
Pyrimidine metabolism	100	1.08111	1.784×10^{-2}
Purine metabolism	154	1.06749	1.8009×10^{-2}
Squamous cell carcinoma			
Respiratory chain and oxidative phosphorylation	74	1.16544	4.60×10^{-6}
Purine metabolism	154	1.03009	7.87×10^{-4}
Tricarboxylic acid cycle	27	1.13055	1.177×10^{-3}
Branched chain amino acids metabolism	55	1.06616	3.688×10^{-3}
Glucose metabolism	53	1.08078	7.449×10^{-3}
Aspartate metabolism	26	1.14841	8.051×10^{-3}
Folate biosynthesis	20	1.17777	1.2205×10^{-2}
Pyrimidine metabolism	100	1.09129	2.0488×10^{-2}
Mannose metabolism	33	1.0791	2.3137×10^{-2}
Amino sugars synthesis	19	1.13317	2.5646×10^{-2}

Table 4. Oncogenes and tumor suppressors significantly affected in lung adenocarcinoma (ADC) and squamous cell carcinoma (SCC)

Name	Description	Fold-change	p-value
Adenocarcinoma			
FOS	v-fos FBJ murine osteosarcoma viral oncogene homolog	-2.02	9.18×10^{-4}
FOSB	FBJ murine osteosarcoma viral oncogene homolog B	-2.14	4.87×10^{-4}
Squamous cell carcinoma			
ECT2	Epithelial cell transforming sequence 2 oncogene	3.59	2.55×10^{-8}
DCUN1D1	DCN1, defective in cullin neddylation 1, domain containing 1 (<i>S. cerevisiae</i>)	2.66	4.00×10^{-7}
JUN	jun oncogene	-2.30	7.39×10^{-9}
FOS	v-fos FBJ murine osteosarcoma viral oncogene homolog	-2.80	7.18×10^{-7}
ROS1	c-ros oncogene 1 , receptor tyrosine kinase	-2.97	8.79×10^{-9}
CXCL2	Chemokine (C-X-C motif) ligand 2	-3.65	2.45×10^{-8}
FOSB	FBJ murine osteosarcoma viral oncogene homolog B	-4.65	1.60×10^{-9}
DLG1	Discs, large homolog 1 (<i>Drosophila</i>)	2.41	3.46×10^{-5}
DLGAP5	Discs, large (<i>Drosophila</i>) homolog-associated protein 5	2.35	4.22×10^{-7}
TGFBR2	Transforming growth factor, beta receptor II (70/80 kDa)	-2.09	1.85×10^{-11}

row publications, but when combined together they provide an unbiased and comprehensive picture of cellular gene expression network. Another critically important power of SNEA is in its ability to find ‘hidden’ regulators, for example genes and proteins for which changes in cancer are not detected on the level of mRNA, but rather on a biologic activity level. This is particularly important for proteins for which activity is regulated at the post-transcriptional level, such

as post-translational protein modification, protein stability, or degradation. The vast majority of cancer signaling pathways are activated or inactivated through phosphorylation of individual protein kinases, an event that is unlikely to be reflected on the level of mRNA measured in gene expression profiling. Similarly, activity of many transcription factors downstream of major signaling cascades is regulated by phosphorylation, and these changes will be overlooked in

traditional gene expression profiling. SNEA can detect such regulators by looking at the changes in downstream targets, rather than the gene/protein itself. Another important advantage of SNEA is its ability to summarize the individual gene expression changes and to project them to the system-level cellular signaling map.

Molecular complexity of ADC and SCC

Our search for key transcriptional regulators involved in differential changes using the ResNet 7 transcriptional network showed uniform involvement of E2F, CTGF, and PDGF in lung cancer pathogenesis. These observations are consistent with previous reports describing the role of CTGF and PDGF in lung cancer progression [20-22]. Our analysis showed that SCC can be uniquely characterized by the involvement of the EGF, IL1F8, and CX3CL1 pathways, while changes in Rb1, miR-200, and EMP2 targets are specific for ADC.

Consistent with the aggressively proliferative phenotype of lung cancer cells, the most significantly affected cellular processes were those involved in the cell cycle and metastasis. The biochemical ‘signature’ pinpoints changes in purine and pyrimidine biosynthesis and energy production pathways, and these changes were seen in both ADC and SCC. Up-regulation of cell-cycle-related genes was more profound in SCC than in ADC. DNA repair genes were also more profoundly up-regulated in SCC. There were no significant changes in apoptotic genes in either type of lung cancer. Surprisingly, we found that all oncogenes in ADC and most oncogenes in SCC were significantly down-regulated, including FOS and FOSB. In SCC, ECT2 and DCUN1D1 were up-regulated. Tumor suppressors were not changed significantly in ADC, whereas in SCC, the significantly changed tumor suppressors were DLG1 and DLGAP5 (elevated), and TGFBR2 (down-regulated).

In conclusion, we found that ADC and SCC subtypes of NSCLC can be characterized by unique gene signatures and distinct molecular pathways. Our data suggest that the gene expression signature of subtypes of lung cancer can be a critical tool for improved characterization of subtypes currently classified based on analysis of histology of tumor samples by light microscopy. Taken together, these data provide a better understanding of the unique molecular

features of NSCLC subtypes, and may open new avenues towards the molecular-based identification of novel therapeutic strategies for NSCLC.

Acknowledgements

We thank Ann Contijoch, Sanofi, for reviewing this paper. Editorial assistance was provided by ArticulateScience Ltd., supported by Sanofi.

Conflict of interest

Valeria Ossovskaya is employee of BiPar Sciences Inc. (subsidiary of Sanofi). Yipeng Wang, Adam Budoff, Gordon Vasant, and Joseph Monforte are employees of AltheaDx Inc. Qiang Xu is former employee of AltheaDx Inc. Alexander Lituev and Olga Potapova are employees of Cureline Inc. Nikolai Daraselia is employee of Ariadne Inc.

Address correspondence to: Dr. Valeria S. Ossovskaya, BiPar Sciences, Inc. (subsidiary of Sanofi), 400 Oyster Point Blvd., Suite 200, South San Francisco, CA 94080 Tel: (650) 615-7019; Fax: (650) 615-7005; E-mail: valeria.ossovskaya@sanofi-aventis.com

References

- [1] Ferlay J, Autier P, Boniol M, Heanue M, Colombet M and Boyle P. Estimates of the cancer incidence and mortality in Europe in 2006. *Ann Oncol* 2007; 18: 581-592.
- [2] Parkin DM, Bray F, Ferlay J and Pisani P. Global cancer statistics, 2002. *CA Cancer J Clin* 2005; 55: 74-108.
- [3] Jemal A, Siegel R, Ward E, Hao Y, Xu J and Thun MJ. Cancer statistics, 2009. *CA Cancer J Clin* 2009; 59: 225-249.
- [4] NCCN. Clinical practice guidelines in oncology: non-small cell lung cancer. NCCN Clinical Practice Guidelines in Oncology, v2 2009.
- [5] Borczuk AC, Toonkel RL and Powell CA. Genomics of lung cancer. *Proc Am Thorac Soc* 2009; 6: 152-158.
- [6] Borczuk AC, Powell CA. Expression profiling and lung cancer development. *Proc Am Thorac Soc* 2007; 4: 127-132.
- [7] Govindan R, Page N, Morgensztern D, Read W, Tierney R, Vlahiotis A, Spitznagel EL and Piccirillo J. Changing epidemiology of small-cell lung cancer in the United States over the last 30 years: analysis of the surveillance, epidemiologic, and end results database. *J Clin Oncol* 2006; 24: 4539-4543.
- [8] Langer CJ, Besse B, Gulaberto A, Brambilla E and Soria JC. The evolving role of histology in

Molecular signature of lung cancers

- the management of advanced non-small cell lung cancer. *J Clin Oncol* 2010; 28: 5311-5320.
- [9] Daraselia N, Yuryev A, Egorov S, Mazo I and Ispolatov I. Automatic extraction of gene ontology annotation and its correlation with clusters in protein network. *BMC Bioinformatics* 2007; 8: 243.
- [10] Novichkova S, Egorov S and Daraselia N. Med-Scan, a natural language processing engine for MEDLINE abstracts. *Bioinformatics* 2011; 19: 1699-1706.
- [11] Sivachenko AY, Yuryev A, Daraselia N and Mazo I. Molecular networks in microarray analysis. *J Bioinform Comput Biol* 2007; 5: 429-456.
- [12] Sivachenko AY, Yuryev A, Daraselia N and Mazo I. Identifying local gene expression patterns in biomolecular networks, pp.180-184, 2005 IEE Computational Systems Bioinformatics Conference - Workshops (CSBW'05), 2005.
- [13] Sivachenko AY, Kalinin A and Yuryev A. Pathway analysis for design of promiscuous drugs and selective drug mixtures. *Curr Drug Discov Technol* 2006; 3: 269-277.
- [14] Yuryev A, Mulyukov Z, Kotelnikova E, Maslov S, Egorov S, Nikitin A, Daraselia N and Mazo I. Automatic pathway building in biological association networks. *BMC Bioinformatics* 2006; 7: 171.
- [15] Yuryev A. In silico pathway analysis: the final frontier towards completely rational drug design. *Expert Opinon Drug Discov* 2008; 3: 867-876.
- [16] Subramanian A, Tamayo P, Mootha VK, Mukherjee S, Ebert BL, Gillette MA, Paulovich A, Pomero SL, Golub TR, Lander ES and Mesirov JP. Gene set enrichment analysis; a knowledge-based approach for interpreting genome-wide expression profiles. *Proc Natl Acad Sci USA* 2005; 102: 15545-15550.
- [17] Bracken CP, Gregory PA, Kolesnikoff N, Bert AG, Wang J, Shannon MF and Goodall GJ. A double-negative feedback loop between ZEB1-SIP1 and the microRNA-200 family regulates epithelial-mesenchymal transition. *Cancer Res* 2008; 68: 7846-7854.
- [18] Wadehra M, Goodlick L and Braun J. The tetraspan protein EMP2 modulates the surface expression of caveolins and glycosylphosphatidyl inositol-linked proteins. *Mol Biol Cell* 2004; 15: 2073-2083.
- [19] Wood RD, Mitchell M, Lindhal T. Human DNA repair genes, 2005. *Mutat Res* 2005; 577: 275-283.
- [20] Chen PP, Li WJ, Wang Y, Zhao S, Li DY, Feng LY, Shi XL, Koeffler HP, Tong XJ and Xie D. Expression of Cyr61, CTGF and WISP-1 correlates with clinical features of lung cancer. *PLoS ONE* 2007; 2: e534.
- [21] Donnem T, Al Saad S, Al Shibli K, Busund LT and Bremnes RM. Co-expression of PDGF-B and VEGFR-3 strongly correlates with lymph node metastasis and poor survival in non-small-cell lung cancer. *Ann Oncol* 2010; 21: 223-231.
- [22] Kinoshita K, Nakagawa K, Hamada J, Hida Y, Tada M, Kondo S and Moriuchi T. Imatinib mesylate inhibits the proliferation-stimulating effect of human lung cancer-associated stromal fibroblasts on lung cancer cells. *Int J Oncol* 2010; 37: 869-877.

Supplementary material

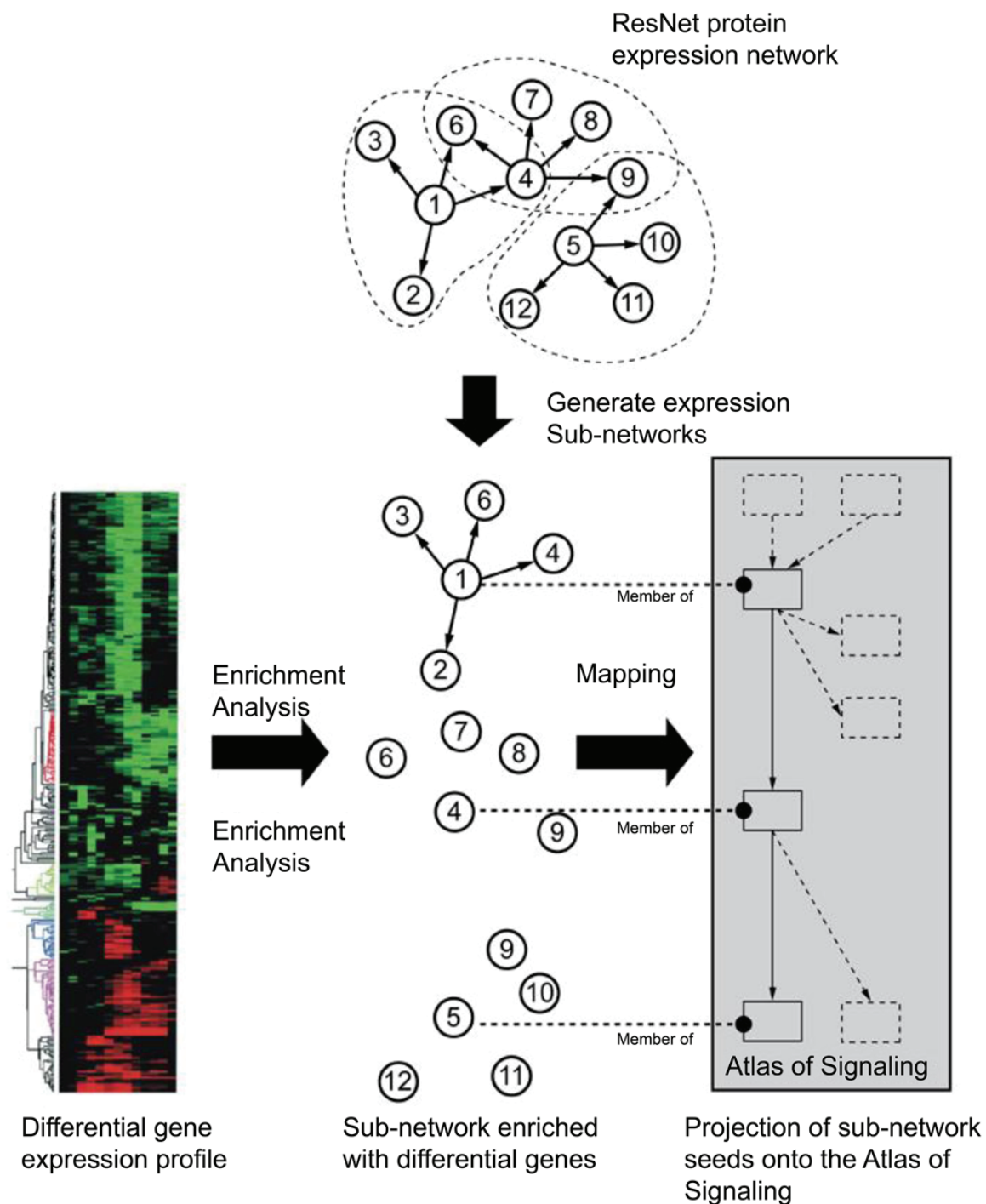


Figure S1. An overview of Sub-Network Enrichment Analysis (SNEA) algorithms

Table S1. Differential expression in DNA repair genes

Name	Description	SCC		ADC	
		fold-change	p-value	fold-change	p-value
RBBP8	Retinoblastoma binding protein 8	2.15	9.61×10^{-7}	1.26	5.34×10^{-2}
PRKDC	Protein kinase, DNA-activated, catalytic polypeptide	2.14	3.89×10^{-7}	1.45	1.10×10^{-3}
SHFM1	Split hand/foot malformation (ectrodactyly) type 1	2.12	1.96×10^{-7}	1.34	1.61×10^{-1}
PCNA	Proliferating cell nuclear antigen	2.01	1.66×10^{-6}	1.43	4.79×10^{-4}
CHEK1	CHK1 checkpoint homolog (<i>S. Pombe</i>)	1.97	1.33×10^{-5}	1.35	1.20×10^{-4}
FANCI	Fanconi anemia, complementation group I	1.84	2.79×10^{-6}	1.29	4.88×10^{-3}
CHAF1A	Chromatin assembly factor 1, subunit A (p150)	1.82	2.55×10^{-7}	1.28	1.52×10^{-4}
EXO1	Exonuclease 1	1.79	7.13×10^{-7}	1.36	4.29×10^{-4}
CHEK2	CHK2 checkpoint homolog (<i>S. Pombe</i>)	1.73	9.38×10^{-6}	1.18	1.62×10^{-2}
APEX1	APEX nuclease (multifunctional DNA repair enzyme) 1	1.73	6.67×10^{-7}	1.32	2.22×10^{-2}
BLM	Bloom syndrome, RecQ helicase-like	1.72	8.70×10^{-6}	1.25	1.41×10^{-4}
POLB	Polymerase (DNA directed), beta	1.59	8.74×10^{-5}	1.28	3.57×10^{-2}
BRCA1	Breast cancer 1, early onset	1.56	2.13×10^{-5}	1.11	1.25×10^{-1}
PMS2	PMS2 postmeiotic segregation increased 2 (<i>S. cerevisiae</i>)	1.54	3.87×10^{-4}	1.21	2.58×10^{-2}
PARP1	Poly (ADP-ribose) polymerase 1	1.54	3.11×10^{-4}	1.23	4.17×10^{-2}
CETN2	Centrin, EF-hand protein, 2	1.52	3.31×10^{-3}	-1.06	7.41×10^{-1}
CDK7	Cyclin-dependent kinase 7	1.50	1.53×10^{-4}	1.09	3.01×10^{-1}
MSH6	mutS homolog 6 (<i>E. Coli</i>)	1.49	1.29×10^{-3}	1.05	6.09×10^{-1}
ATR	Ataxia telangiectasia and Rad3 related	1.46	1.50×10^{-4}	1.10	2.66×10^{-1}
UBE2V2	Ubiquitin-conjugating enzyme E2 variant 2	1.45	2.00×10^{-5}	1.11	1.28×10^{-1}

<i>FEN1</i>	Flap structure-specific endonuclease 1	1.45	4.79×10^{-7}	1.39	4.18×10^{-7}
<i>PARP2</i>	Poly (ADP-ribose) polymerase 2	1.44	2.05×10^{-3}	1.06	5.74×10^{-1}
<i>FANCD2</i>	Fanconi anemia, complementation group D2	1.44	6.33×10^{-6}	1.09	1.90×10^{-1}
<i>FANCL</i>	Fanconi anemia, complementation group L	1.41	3.93×10^{-2}	-1.08	5.57×10^{-1}
<i>RAD54B</i>	RAD54 homolog B (<i>S. cerevisiae</i>)	1.41	4.37×10^{-6}	1.15	4.16×10^{-3}
<i>GTF2H3</i>	General transcription factor IIH, polypeptide 3, 34 kDa	1.38	1.58×10^{-3}	1.19	3.65×10^{-3}
<i>TDG</i>	Thymine-DNA glycosylase	1.38	1.58×10^{-3}	1.16	5.83×10^{-2}
<i>XRCC6</i>	X-ray repair complementing defective repair in Chinese hamster cells 6	1.37	1.98×10^{-3}	1.07	3.63×10^{-1}
<i>UNG</i>	Uracil-DNA glycosylase	1.36	1.67×10^{-5}	1.13	5.20×10^{-2}
<i>MSH2</i>	mutS homolog 2, colon cancer, nonpolyposis type 1 (<i>E. Coli</i>)	1.36	9.78×10^{-3}	1.26	1.49×10^{-3}
<i>DDB1</i>	Damage-specific DNA binding protein 1, 127 kDa	1.36	2.18×10^{-3}	1.12	2.29×10^{-1}
<i>OBFC2B</i>	Oligonucleotide/oligosaccharide-binding fold containing 2B	1.35	1.63×10^{-4}	1.15	9.60×10^{-3}
<i>XRCC4</i>	X-ray repair complementing defective repair in Chinese hamster cells 4	1.34	3.81×10^{-3}	1.13	1.12×10^{-1}
<i>TDP1</i>	Tyrosyl-DNA phosphodiesterase 1	1.29	1.75×10^{-4}	1.13	2.73×10^{-2}
<i>PALB2</i>	Partner and localizer of BRCA2	1.28	1.88×10^{-3}	1.05	3.43×10^{-1}
<i>GTF2H1</i>	General transcription factor IIH, polypeptide 1, 62 kDa	1.27	5.39×10^{-2}	1.13	1.53×10^{-1}
<i>PMS2L3</i>	Postmeiotic segregation increased 2-like 3	1.27	2.48×10^{-2}	1.28	1.76×10^{-2}
<i>APTX</i>	Aprataxin	1.26	2.40×10^{-3}	1.09	1.33×10^{-1}
<i>MNAT1</i>	Menage a trois homolog 1, cyclin H assembly factor (<i>X. laevis</i>)	1.26	1.54×10^{-2}	-1.01	8.98×10^{-1}
<i>RAD51</i>	RAD51 homolog (RecA homolog, <i>E. Coli</i>) (<i>S. cerevisiae</i>)	1.25	4.56×10^{-3}	1.14	2.94×10^{-2}
<i>FANCF</i>	Fanconi anemia,	1.24	3.57×10^{-3}	1.11	5.48×10^{-2}

	complementation group F				
<i>DCLRE1A</i>	DNA cross-link repair 1A (PSO2 homolog, <i>S. cerevisiae</i>)	1.24	2.93×10^{-3}	1.19	1.59×10^{-3}
<i>RAD51C</i>	RAD51 homolog C (<i>S. cerevisiae</i>)	1.24	3.84×10^{-3}	1.06	3.43×10^{-1}
<i>RECQL</i>	RecQ protein-like (DNA helicase Q1-like)	1.24	3.15×10^{-2}	1.04	5.70×10^{-1}
<i>WRN</i>	Werner syndrome, RecQ helicase-like	1.23	7.64×10^{-2}	-1.28	1.76×10^{-3}
<i>XRCC5</i>	X-ray repair complementing defective repair in Chinese hamster cells 5 (double-strand-break rejoining)	1.22	2.27×10^{-2}	-1.02	8.53×10^{-1}
<i>RAD18</i>	RAD18 homolog (<i>S. cerevisiae</i>)	1.22	1.58×10^{-4}	1.12	1.57×10^{-2}
<i>ERCC6</i>	Excision repair cross-complementing rodent repair deficiency, complementation group 6	1.20	1.10×10^{-2}	-1.03	6.42×10^{-1}
<i>POLQ</i>	Polymerase (DNA directed), theta	1.20	1.45×10^{-2}	1.05	3.89×10^{-1}
<i>CLK2</i>	CDC-like kinase 2	1.19	6.15×10^{-3}	1.27	1.55×10^{-4}
<i>FANCE</i>	Fanconi anemia, complementation group E	1.18	4.80×10^{-3}	1.04	3.84×10^{-1}
<i>FANCA</i>	Fanconi anemia, complementation group A	1.18	2.57×10^{-3}	1.15	3.99×10^{-3}
<i>NUDT1</i>	nudix (nucleoside diphosphate linked moiety X)-type motif 1	1.18	1.23×10^{-3}	1.15	1.33×10^{-2}
<i>DUT</i>	Deoxyuridine triphosphatase	1.18	4.96×10^{-3}	1.08	2.18×10^{-1}
<i>TP53</i>	tumor protein p53	1.18	6.27×10^{-2}	1.09	1.88×10^{-1}
<i>RAD54L</i>	RAD54-like (<i>S. cerevisiae</i>)	1.18	5.95×10^{-3}	1.16	9.38×10^{-3}
<i>EME1</i>	Essential meiotic endonuclease 1 homolog 1 (<i>S. Pombe</i>)	1.17	2.57×10^{-3}	1.14	3.56×10^{-2}
<i>ERCC1</i>	Excision repair cross-complementing rodent repair deficiency, complementation group 1 (includes overlapping antisense sequence)	1.17	6.47×10^{-4}	1.03	5.51×10^{-1}
<i>RAD23B</i>	RAD23 homolog B (<i>S. cerevisiae</i>)	1.17	7.37×10^{-2}	1.09	2.50×10^{-1}
<i>BRCA2</i>	breast cancer 2, early onset	1.17	1.61×10^{-2}	1.02	6.07×10^{-1}

<i>SMUG1</i>	single-strand-selective monofunctional uracil-DNA glycosylase 1	1.16	1.41×10^{-2}	1.12	3.81×10^{-2}
<i>MSH5</i>	mutS homolog 5 (<i>E. Coli</i>)	1.16	2.48×10^{-3}	1.10	7.79×10^{-2}
<i>NBN</i>	Nibrin	1.16	2.26×10^{-1}	1.10	3.12×10^{-1}
<i>FANCG</i>	Fanconi anemia, complementation group G	1.16	5.29×10^{-4}	1.10	7.89×10^{-2}
<i>LIG3</i>	Ligase III, DNA, ATP-dependent	1.16	2.82×10^{-2}	1.15	6.57×10^{-3}
<i>RAD1</i>	RAD1 homolog (<i>S. Pombe</i>)	1.15	3.82×10^{-2}	1.14	5.71×10^{-2}
<i>RAD50</i>	RAD50 homolog (<i>S. cerevisiae</i>)	1.15	3.50×10^{-1}	-1.14	3.96×10^{-1}
<i>FANCB</i>	Fanconi anemia, complementation group B	1.14	4.52×10^{-2}	1.17	1.22×10^{-2}
<i>DDB2</i>	Damage-specific DNA binding protein 2, 48 kDa	1.14	3.45×10^{-2}	1.15	4.07×10^{-3}
<i>GTF2H5</i>	General transcription factor IIH, polypeptide 5	1.14	7.73×10^{-2}	1.11	2.18×10^{-1}
<i>RAD23A</i>	RAD23 homolog A (<i>S. cerevisiae</i>)	1.13	1.05×10^{-1}	1.03	6.54×10^{-1}
<i>POLE</i>	Polymerase (DNA directed), epsilon	1.12	2.41×10^{-2}	1.05	3.21×10^{-1}
<i>XRCC1</i>	X-ray repair complementing defective repair in Chinese hamster cells 1	1.11	3.77×10^{-2}	1.13	2.74×10^{-3}
<i>MRE11A</i>	MRE11 meiotic recombination 11 homolog A (<i>S. cerevisiae</i>)	1.10	4.23×10^{-1}	1.05	6.12×10^{-1}
<i>FANCM</i>	Fanconi anemia, complementation group M	1.10	7.10×10^{-2}	-1.02	6.83×10^{-1}
<i>APEX2</i>	APEX nuclease (apurinic/apyrimidinic endonuclease) 2	1.10	5.71×10^{-2}	1.05	2.46×10^{-1}
<i>PMS1</i>	PMS1 postmeiotic segregation increased 1 (<i>S. cerevisiae</i>)	1.10	7.01×10^{-2}	1.09	6.87×10^{-2}
<i>LIG1</i>	Ligase I, DNA, ATP-dependent	1.09	4.08×10^{-2}	1.12	5.11×10^{-3}
<i>NEIL3</i>	nei endonuclease VIII-like 3 (<i>E. Coli</i>)	1.09	9.13×10^{-2}	1.12	6.20×10^{-2}
<i>RPA1</i>	Replication protein A1, 70 kDa	1.08	2.72×10^{-2}	1.08	4.27×10^{-2}
<i>ALKBH2</i>	alkB, alkylation repair homolog 2	1.08	1.96×10^{-1}	1.02	7.80×10^{-1}

	(<i>E. Coli</i>)				
ALKBH3	alkB, alkylation repair homolog 3 (<i>E. Coli</i>)	1.08	1.79×10^{-1}	1.08	2.22×10^{-1}
HUS1	HUS1 checkpoint homolog (<i>S. Pombe</i>)	1.08	2.59×10^{-1}	1.03	7.19×10^{-1}
UBE2A	Ubiquitin-conjugating enzyme E2A (RAD6 homolog)	1.08	2.09×10^{-1}	-1.01	8.50×10^{-1}
ERCC4	Excision repair cross-complementing rodent repair deficiency, complementation group 4	1.07	2.51×10^{-1}	1.06	3.21×10^{-1}
MBD4	Methyl-CpG binding domain protein 4	1.07	4.14×10^{-1}	1.11	5.74×10^{-2}
MAD2L2	MAD2 mitotic arrest deficient-like 2 (yeast)	1.07	2.13×10^{-1}	1.12	3.10×10^{-2}
LIG4	Ligase IV, DNA, ATP-dependent	1.06	3.15×10^{-1}	1.11	7.92×10^{-2}
RAD52	RAD52 homolog (<i>S. cerevisiae</i>)	1.06	3.06×10^{-1}	-1.05	2.82×10^{-1}
MDC1	Mediator of DNA damage checkpoint 1	1.06	4.24×10^{-1}	1.03	6.25×10^{-1}
MUTYH	mutY homolog (<i>E. Coli</i>)	1.06	2.57×10^{-1}	1.05	3.47×10^{-1}
RPA3	Replication protein A3, 14 kDa	1.06	2.83×10^{-1}	1.14	5.66×10^{-3}
POLH	Polymerase (DNA directed), eta	1.06	4.73×10^{-1}	1.11	2.02×10^{-1}
POLN	Polymerase (DNA directed) nu	1.05	2.92×10^{-1}	1.12	1.98×10^{-2}
GTF2H4	General transcription factor IIH, polypeptide 4, 52 kDa	1.05	1.64×10^{-1}	1.06	2.92×10^{-1}
DCLRE1C	DNA cross-link repair 1C (PSO2 homolog, <i>S. cerevisiae</i>)	1.05	4.68×10^{-1}	1.20	1.05×10^{-3}
XAB2	XPA binding protein 2	1.04	4.75×10^{-1}	1.07	1.75×10^{-1}
H2AFX	H2A histone family, member X	1.04	4.13×10^{-1}	1.25	4.58×10^{-6}
ERCC3	Excision repair cross-complementing rodent repair deficiency, complementation group 3 (xeroderma pigmentosum group B complementing)	1.04	6.20×10^{-1}	-1.05	5.19×10^{-1}
RAD51L1	RAD51-like 1 (<i>S. cerevisiae</i>)	1.04	5.92×10^{-1}	1.06	3.94×10^{-1}
XRCC3	X-ray repair complementing defective repair in Chinese	1.04	4.91×10^{-1}	1.18	2.41×10^{-3}

	hamster cells 3				
RPA2	replication protein A2, 32 kDa	1.04	6.87×10^{-1}	1.02	8.38×10^{-1}
ATM	ataxia telangiectasia mutated	1.04	7.26×10^{-1}	-1.21	7.93×10^{-2}
RAD17	RAD17 homolog (<i>S. Pombe</i>)	1.04	6.98×10^{-1}	1.21	1.44×10^{-2}
REV1	REV1 homolog (<i>S. cerevisiae</i>)	1.03	6.98×10^{-1}	-1.09	2.49×10^{-1}
RAD51L3	RAD51-like 3 (<i>S. cerevisiae</i>)	1.03	5.07×10^{-1}	1.06	2.89×10^{-1}
UBE2B	Ubiquitin-conjugating enzyme E2B (RAD6 homolog)	1.03	6.85×10^{-1}	-1.20	7.78×10^{-2}
RDM1	RAD52 motif 1	1.02	6.46×10^{-1}	1.16	4.44×10^{-3}
MSH4	mutS homolog 4 (<i>E. Coli</i>)	1.02	7.35×10^{-1}	1.00	9.38×10^{-1}
RECQL4	RecQ protein-like 4	1.02	6.92×10^{-1}	1.12	3.02×10^{-2}
ERCC2	Excision repair cross-complementing rodent repair deficiency, complementation group 2	1.01	8.80×10^{-1}	1.18	8.45×10^{-4}
NTHL1	nth endonuclease III-like 1 (<i>E. Coli</i>)	1.00	9.79×10^{-1}	1.07	1.54×10^{-1}
POLM	Polymerase (DNA directed), mu	-1.00	9.79×10^{-1}	1.07	1.53×10^{-1}
MSH3	mutS homolog 3 (<i>E. Coli</i>)	-1.00	9.80×10^{-1}	-1.00	9.47×10^{-1}
ERCC5	Excision repair cross-complementing rodent repair deficiency, complementation group 5	-1.00	9.70×10^{-1}	-1.32	2.85×10^{-3}
EME2	Essential meiotic endonuclease 1 homolog 2 (<i>S. Pombe</i>)	-1.01	8.17×10^{-1}	-1.02	6.86×10^{-1}
PNKP	Polynucleotide kinase 3'-phosphatase	-1.01	7.46×10^{-1}	1.14	4.45×10^{-3}
XPA	Xeroderma pigmentosum, complementation group A	-1.01	8.65×10^{-1}	-1.08	2.43×10^{-1}
POLD1	Polymerase (DNA directed), delta 1, catalytic subunit 125 kDa	-1.02	7.40×10^{-1}	1.05	3.27×10^{-1}
TREX2	Three prime repair exonuclease 2	-1.02	6.83×10^{-1}	1.10	9.88×10^{-2}
POLL	Polymerase (DNA directed), lambda	-1.02	6.14×10^{-1}	1.03	6.11×10^{-1}
MMS19	MMS19 nucleotide excision repair	-1.02	5.25×10^{-1}	-1.03	4.03×10^{-1}

	homolog (<i>S. cerevisiae</i>)				
<i>MPG</i>	N-methylpurine-DNA glycosylase	-1.03	4.49×10^{-1}	1.11	2.26×10^{-3}
<i>RAD9A</i>	RAD9 homolog A (<i>S. Pombe</i>)	-1.03	5.52×10^{-1}	1.06	2.13×10^{-1}
<i>TREX1</i>	Three prime repair exonuclease 1	-1.03	4.99×10^{-1}	-1.06	2.04×10^{-1}
<i>MUS81</i>	MUS81 endonuclease homolog (<i>S. cerevisiae</i>)	-1.04	4.33×10^{-1}	1.10	3.02×10^{-2}
<i>OGG1</i>	8-oxoguanine DNA glycosylase	-1.05	3.02×10^{-1}	1.08	8.32×10^{-2}
<i>RECQL5</i>	RecQ protein-like 5	-1.05	2.99×10^{-1}	1.11	4.41×10^{-2}
<i>POLI</i>	Polymerase (DNA directed) iota	-1.05	6.10×10^{-1}	-1.12	3.06×10^{-1}
<i>DCLRE1B</i>	DNA cross-link repair 1B (PSO2 homolog, <i>S. cerevisiae</i>)	-1.06	4.75×10^{-1}	1.11	1.35×10^{-1}
<i>DMC1</i>	DMC1 dosage suppressor of mck1 homolog, meiosis-specific homologous recombination (yeast)	-1.06	2.82×10^{-1}	1.07	2.07×10^{-1}
<i>NEIL2</i>	nei like 2 (<i>E. Coli</i>)	-1.07	1.90×10^{-1}	1.11	3.17×10^{-2}
<i>POLK</i>	Polymerase (DNA directed) kappa	-1.07	5.64×10^{-1}	-1.24	3.58×10^{-2}
<i>ERCC8</i>	Excision repair cross-complementing rodent repair deficiency, complementation group 8	-1.09	1.59×10^{-1}	1.05	3.57×10^{-1}
<i>MGMT</i>	O-6-methylguanine-DNA methyltransferase	-1.09	8.14×10^{-2}	1.05	1.79×10^{-1}
<i>UBE2N</i>	Ubiquitin-conjugating enzyme E2N (UBC13 homolog, yeast)	-1.09	1.84×10^{-1}	-1.11	8.47×10^{-2}
<i>GTF2H2</i>	General transcription factor IIH, polypeptide 2, 44 kDa	-1.10	5.17×10^{-1}	-1.20	2.56×10^{-1}
<i>Hel308</i>	Helicase, POLQ-like	-1.11	1.45×10^{-1}	-1.05	3.62×10^{-1}
<i>SP011</i>	SPO11 meiotic protein covalently bound to DSB homolog (<i>S. cerevisiae</i>)	-1.11	1.26×10^{-1}	1.01	7.93×10^{-1}
<i>MLH1</i>	mutL homolog 1, colon cancer, nonpolyposis type 2 (<i>E. Coli</i>)	-1.12	1.27×10^{-1}	-1.23	2.00×10^{-3}
<i>POLG</i>	polymerase (DNA directed), gamma	-1.12	1.54×10^{-2}	1.03	5.51×10^{-1}
<i>RRM2B</i>	Ribonucleotide reductase M2 B	-1.13	8.62×10^{-2}	1.09	2.92×10^{-1}

	(TP53 inducible)				
<i>RPA4</i>	Replication protein A4, 34 kDa	-1.14	2.69×10^{-2}	-1.11	4.93×10^{-2}
<i>NEIL1</i>	nei endonuclease VIII-like 1 (<i>E. Coli</i>)	-1.14	2.79×10^{-2}	-1.04	4.78×10^{-1}
<i>XPC</i>	Xeroderma pigmentosum, complementation group C	-1.14	2.71×10^{-2}	-1.11	1.05×10^{-1}
<i>MLH3</i>	mutL homolog 3 (<i>E. Coli</i>)	-1.16	1.25×10^{-2}	-1.10	1.44×10^{-1}
<i>FANCC</i>	Fanconi anemia, complementation group C	-1.21	3.49×10^{-3}	-1.14	2.08×10^{-2}
<i>REV3L</i>	REV3-like, catalytic subunit of DNA polymerase zeta (yeast)	-1.25	1.14×10^{-2}	-1.19	3.02×10^{-2}
<i>PER1</i>	Period homolog 1 (<i>Drosophila</i>)	-1.37	5.61×10^{-6}	-1.19	7.80×10^{-3}
<i>CCNH</i>	Cyclin H	-1.69	1.94×10^{-4}	-1.50	1.66×10^{-2}
<i>A730011L_01Rik</i>	Hypothetical protein FLJ35220				
<i>GEN1</i>	Gen homolog 1, endonuclease (<i>Drosophila</i>)				
<i>PMS2L4</i>	Postmeiotic segregation increased 2-like 4 pseudogene				
<i>ATRIP</i>	ATR interacting protein				
<i>XRCC2</i>	X-ray repair complementing defective repair in Chinese hamster cells 2				
<i>C19orf40</i>	Chromosome 19 open reading frame 40				

Table S2. Differential changes in cell cycle genes

Name	Description	SCC		ADC	
		fold-change	p-value	fold-change	p-value
<i>TOP2A</i>	Topoisomerase (DNA) II alpha 170 kDa	5.43	1.23×10^{-11}	2.92	7.95×10^{-9}
<i>CCNB1</i>	Cyclin B1	2.75	6.97×10^{-8}	1.56	4.82×10^{-5}
<i>MELK</i>	Maternal embryonic leucine zipper kinase	2.67	1.75×10^{-7}	1.45	3.21×10^{-6}
<i>MAD2L1</i>	MAD2 mitotic arrest deficient-like 1 (yeast)	2.63	4.69×10^{-9}	1.38	2.05×10^{-4}
<i>SFN</i>	Stratifin	2.60	1.94×10^{-7}	1.43	1.28×10^{-5}
<i>CDC6</i>	Cell division cycle 6 homolog (<i>S. cerevisiae</i>)	2.54	3.24×10^{-9}	1.54	2.40×10^{-4}
<i>ASPM</i>	asp (abnormal spindle) homolog, microcephaly associated (<i>Drosophila</i>)	2.48	1.45×10^{-7}	1.57	7.97×10^{-5}
<i>TOPBP1</i>	Topoisomerase (DNA) II binding protein 1	2.02	5.03×10^{-6}	1.18	4.88×10^{-2}
<i>CHEK1</i>	CHK1 checkpoint homolog (<i>S. Pombe</i>)	1.97	1.33×10^{-5}	1.35	1.20×10^{-4}
<i>CCNB2</i>	Cyclin B2	1.93	1.69×10^{-6}	1.30	5.87×10^{-4}
<i>CDC2</i>	Cell division cycle 2, G1 to S and G2 to M	1.84	2.57×10^{-6}	1.37	7.20×10^{-5}
<i>EZH2</i>	Enhancer of zeste homolog 2 (<i>Drosophila</i>)	1.78	6.05×10^{-8}	1.24	8.23×10^{-3}
<i>CHEK2</i>	CHK2 checkpoint homolog (<i>S. Pombe</i>)	1.73	9.38×10^{-6}	1.18	1.62×10^{-2}
<i>CDK4</i>	Cyclin-dependent kinase 4	1.70	3.64×10^{-6}	1.34	3.85×10^{-3}
<i>GMNN</i>	Geminin, DNA replication inhibitor	1.65	1.07×10^{-4}	1.16	5.31×10^{-2}
<i>NAE1</i>	NEDD8 activating enzyme E1 subunit 1	1.59	1.64×10^{-3}	1.10	3.85×10^{-1}
<i>BRCA1</i>	Breast cancer 1, early onset	1.56	2.13×10^{-5}	1.11	1.25×10^{-1}
<i>CDK6</i>	Cyclin-dependent kinase 6	1.47	2.86×10^{-3}	-1.03	6.09×10^{-1}
<i>ATR</i>	Ataxia telangiectasia and Rad3 related	1.46	1.50×10^{-4}	1.10	2.66×10^{-1}

<i>FANCD2</i>	Fanconi anemia, complementation group D2	1.44	6.33×10^{-6}	1.09	1.90×10^{-1}
<i>HDAC1</i>	Histone deacetylase 1	1.44	1.11×10^{-3}	1.12	3.54×10^{-1}
<i>MSH2</i>	mutS homolog 2, colon cancer, nonpolyposis type 1 (<i>E. Coli</i>)	1.36	9.78×10^{-3}	1.26	1.49×10^{-3}
<i>BIRC5</i>	Baculoviral IAP repeat-containing 5	1.35	1.93×10^{-7}	1.26	1.52×10^{-4}
<i>BARD1</i>	BRCA1 associated RING domain 1	1.33	9.99×10^{-4}	-1.04	3.95×10^{-1}
<i>CDKN2A</i>	Cyclin-dependent kinase inhibitor 2A (melanoma, p16, inhibits CDK4)	1.32	2.06×10^{-2}	1.26	1.15×10^{-3}
<i>RAD51</i>	RAD51 homolog (RecA homolog, <i>E. Coli</i>) (<i>S. cerevisiae</i>)	1.25	4.56×10^{-3}	1.14	2.94×10^{-2}
<i>TBPL1</i>	TBP-like 1	1.23	1.50×10^{-2}	-1.07	3.51×10^{-1}
<i>RINT1</i>	RAD50 interactor 1	1.21	4.38×10^{-3}	1.03	5.78×10^{-1}
<i>FANCA</i>	Fanconi anemia, complementation group A	1.18	2.57×10^{-3}	1.15	3.99×10^{-3}
<i>TP53</i>	Tumor protein p53	1.18	6.27×10^{-2}	1.09	1.88×10^{-1}
<i>CDC25A</i>	Cell division cycle 25 homolog A (<i>S. Pombe</i>)	1.17	1.92×10^{-3}	1.05	5.00×10^{-1}
<i>BRCA2</i>	Breast cancer 2, early onset	1.17	1.61×10^{-2}	1.02	6.07×10^{-1}
<i>NBN</i>	Nibrin	1.16	2.26×10^{-1}	1.10	3.12×10^{-1}
<i>RAD50</i>	RAD50 homolog (<i>S. cerevisiae</i>)	1.15	3.50×10^{-1}	-1.14	3.96×10^{-1}
<i>LIMK1</i>	LIM domain kinase 1	1.15	1.34×10^{-3}	1.20	1.67×10^{-3}
<i>MAPK14</i>	Mitogen-activated protein kinase 14	1.14	2.18×10^{-1}	1.03	8.05×10^{-1}
<i>TAOK1</i>	TAO kinase 1	1.13	3.32×10^{-1}	-1.15	3.06×10^{-1}
<i>CDK5</i>	Cyclin-dependent kinase 5	1.12	6.26×10^{-2}	1.26	6.48×10^{-4}
<i>TP53BP1</i>	Tumor protein p53 binding protein 1	1.12	8.23×10^{-2}	1.02	8.03×10^{-1}
<i>POLE</i>	Polymerase (DNA directed), epsilon	1.12	2.41×10^{-2}	1.05	3.21×10^{-1}
<i>MRE11A</i>	MRE11 meiotic recombination 11 homolog A (<i>S. cerevisiae</i>)	1.10	4.23×10^{-1}	1.05	6.12×10^{-1}

<i>ETV6</i>	ets variant 6	1.10	3.89×10^{-1}	1.14	7.57×10^{-2}
<i>E2F1</i>	E2F transcription factor 1	1.08	7.91×10^{-2}	1.21	9.59×10^{-3}
<i>HUS1</i>	HUS1 checkpoint homolog (<i>S. Pombe</i>)	1.08	2.59×10^{-1}	1.03	7.19×10^{-1}
<i>GADD45A</i>	Growth arrest and DNA-damage-inducible, alpha	1.07	5.45×10^{-1}	-1.00	9.99×10^{-1}
<i>CDC25B</i>	Cell division cycle 25 homolog B (<i>S. Pombe</i>)	1.07	3.34×10^{-1}	1.06	4.34×10^{-1}
<i>MDC1</i>	Mediator of DNA damage checkpoint 1	1.06	4.24×10^{-1}	1.03	6.25×10^{-1}
<i>TOP2B</i>	topoisomerase (DNA) II beta 180 kDa	1.06	6.39×10^{-1}	-1.29	3.22×10^{-2}
<i>UBA3</i>	Ubiquitin-like modifier activating enzyme 3	1.05	5.31×10^{-1}	1.02	7.93×10^{-1}
<i>TP73</i>	Tumor protein p73	1.05	2.53×10^{-1}	1.06	1.64×10^{-1}
<i>CDK2</i>	Cyclin-dependent kinase 2	1.05	5.94×10^{-1}	-1.09	2.64×10^{-1}
<i>DCLRE1C</i>	DNA cross-link repair 1C (PSO2 homolog, <i>S. cerevisiae</i>)	1.05	4.68×10^{-1}	1.20	1.05×10^{-3}
<i>H2AFX</i>	H2A histone family, member X	1.04	4.13×10^{-1}	1.25	4.58×10^{-6}
<i>ATM</i>	ataxia telangiectasia mutated	1.04	7.26×10^{-1}	-1.21	7.93×10^{-2}
<i>RAD17</i>	RAD17 homolog (<i>S. Pombe</i>)	1.04	6.98×10^{-1}	1.21	1.44×10^{-2}
<i>TRAF2</i>	TNF receptor-associated factor 2	1.02	6.59×10^{-1}	1.06	1.34×10^{-1}
<i>UIMC1</i>	Ubiquitin interaction motif containing 1	1.02	7.46×10^{-1}	1.09	1.30×10^{-1}
<i>MAPKAPK2</i>	Mitogen-activated protein kinase-activated protein kinase 2	1.01	7.91×10^{-1}	1.02	7.06×10^{-1}
<i>CDC25C</i>	Cell division cycle 25 homolog C (<i>S. Pombe</i>)	1.01	8.74×10^{-1}	1.08	1.72×10^{-1}
<i>TERF1</i>	Telomeric repeat binding factor (NIMA-interacting) 1	1.01	9.26×10^{-1}	-1.02	8.44×10^{-1}
<i>HDAC4</i>	Histone deacetylase 4	1.01	8.64×10^{-1}	1.02	5.65×10^{-1}
<i>MAP2K2</i>	Mitogen-activated protein kinase kinase 2	1.00	9.69×10^{-1}	1.19	8.11×10^{-3}
<i>SPDYA</i>	Speedy homolog A (<i>Xenopus</i>)	-1.01	8.79×10^{-1}	1.09	9.73×10^{-2}

	Iaevis)				
<i>CEP164</i>	Centrosomal protein 164 kDa	-1.01	8.19×10^{-1}	1.00	9.67×10^{-1}
<i>CDKN1B</i>	Cyclin-dependent kinase inhibitor 1B (p27, Kip1)	-1.01	9.27×10^{-1}	-1.09	3.39×10^{-1}
<i>PPP5C</i>	Protein phosphatase 5, catalytic subunit	-1.01	8.02×10^{-1}	1.05	2.05×10^{-1}
<i>CDKN2B</i>	Cyclin-dependent kinase inhibitor 2B (p15, inhibits CDK4)	-1.01	8.38×10^{-1}	1.20	3.78×10^{-3}
<i>FAM175A</i>	Family with sequence similarity 175, member A	-1.02	7.51×10^{-1}	-1.02	7.81×10^{-1}
<i>RAD9A</i>	RAD9 homolog A (<i>S. Pombe</i>)	-1.03	5.52×10^{-1}	1.06	2.13×10^{-1}
<i>CDT1</i>	Chromatin licensing and DNA replication factor 1	-1.03	6.54×10^{-1}	1.18	1.91×10^{-2}
<i>HMGN1</i>	High-mobility group nucleosome binding domain 1	-1.04	3.83×10^{-1}	1.18	5.14×10^{-3}
<i>PPP2CB</i>	Protein phosphatase 2 (formerly 2A), catalytic subunit, beta isoform	-1.06	6.49×10^{-1}	-1.30	2.75×10^{-2}
<i>MCPH1</i>	Microcephalin 1	-1.07	2.65×10^{-1}	-1.00	9.96×10^{-1}
<i>MAPK1</i>	Mitogen-activated protein kinase 1	-1.08	4.32×10^{-1}	-1.26	1.93×10^{-2}
<i>BTG3</i>	BTG family, member 3	-1.09	4.16×10^{-1}	-1.07	4.18×10^{-1}
<i>MLH1</i>	mutL homolog 1, colon cancer, nonpolyposis type 2 (<i>E. Coli</i>)	-1.12	1.27×10^{-1}	-1.23	2.00×10^{-3}
<i>CCNG1</i>	Cyclin G1	-1.14	2.93×10^{-1}	-1.01	9.02×10^{-1}
<i>CDKN1A</i>	Cyclin-dependent kinase inhibitor 1A (p21, Cip1)	-1.16	1.18×10^{-1}	1.01	9.32×10^{-1}
<i>PPM1D</i>	Protein phosphatase 1D magnesium-dependent, delta isoform	-1.20	9.29×10^{-3}	-1.04	3.42×10^{-1}
<i>WEE1</i>	WEE1 homolog (<i>S. Pombe</i>)	-1.21	3.05×10^{-1}	-1.25	2.52×10^{-1}
<i>FANCC</i>	Fanconi anemia, complementation group C	-1.21	3.49×10^{-3}	-1.14	2.08×10^{-2}
<i>MAPK3</i>	Mitogen-activated protein kinase 3	-1.23	1.58×10^{-4}	-1.08	2.10×10^{-1}
<i>PTGS2</i>	Prostaglandin-endoperoxide synthase 2 (prostaglandin G/H synthase and cyclooxygenase)	-1.72	1.98×10^{-2}	-1.39	5.63×10^{-2}

<i>KLF4</i>	Kruppel-like factor 4 (gut)	-2.31	1.83×10^{-9}	-2.54	5.38×10^{-11}
<i>CAV1</i>	Caveolin 1, caveolae protein, 22 kDa	-4.24	2.78×10^{-10}	-4.80	3.59×10^{-12}
<i>ATRIP</i>	ATR interacting protein				

Table S3. Differential changes in apoptosis genes

Name	Description	SCC		ADC	
		fold-change	p-value	fold-change	p-value
<i>Bim</i>	BCL2-like 11 (apoptosis facilitator)	1.56	6.19×10^{-6}	1.04	4.42×10^{-1}
CYCS	Cytochrome c, somatic	1.49	1.46×10^{-3}	1.10	4.69×10^{-1}
<i>ATR</i>	Ataxia telangiectasia and Rad3 related	1.46	1.50×10^{-4}	1.10	2.66×10^{-1}
CAPN1	Calpain 1, (mu/l) large subunit	1.42	1.09×10^{-7}	1.21	1.46×10^{-3}
<i>BIK</i>	BCL2-interacting killer (apoptosis-inducing)	1.38	4.47×10^{-6}	1.21	1.73×10^{-3}
CASP3	Caspase 3, apoptosis-related cysteine peptidase	1.37	1.95×10^{-4}	1.08	2.50×10^{-1}
<i>BIRC5</i>	Baculoviral IAP repeat-containing 5	1.35	1.93×10^{-7}	1.26	1.52×10^{-4}
<i>BAG1</i>	BCL2-associated athanogene	1.23	1.19×10^{-1}	-1.08	4.39×10^{-1}
<i>BIRC4</i>	X-linked inhibitor of apoptosis	1.22	1.26×10^{-2}	-1.01	9.11×10^{-1}
<i>TP53</i>	Tumor protein p53	1.18	6.27×10^{-2}	1.09	1.88×10^{-1}
<i>DFFA</i>	DNA fragmentation factor, 45 kDa, alpha polypeptide	1.18	2.40×10^{-2}	1.09	1.07×10^{-1}
<i>AIFM1</i>	Apoptosis-inducing factor, mitochondrion-associated, 1	1.15	5.22×10^{-2}	1.09	1.77×10^{-1}
<i>BAK1</i>	BCL2-antagonist/killer 1	1.13	1.08×10^{-1}	1.06	6.30×10^{-1}
<i>ENDOG</i>	Endonuclease G	1.12	5.69×10^{-3}	1.11	6.11×10^{-2}
<i>BAX</i>	BCL2-associated X protein	1.10	5.67×10^{-2}	1.21	4.78×10^{-4}
<i>GZMK</i>	Granzyme K (granzyme 3; tryptase II)	1.08	5.59×10^{-1}	-1.17	2.67×10^{-1}
<i>DIABLO</i>	Diablo homolog (<i>Drosophila</i>)	1.08	2.01×10^{-1}	1.09	1.01×10^{-1}
<i>CASP6</i>	Caspase 6, apoptosis-related cysteine peptidase	1.07	4.09×10^{-1}	1.16	7.90×10^{-2}
<i>MDM2</i>	Mdm2 p53 binding protein homolog (mouse)	1.05	5.56×10^{-1}	-1.04	8.03×10^{-1}
<i>GZMB</i>	Granzyme B (granzyme 2, cytotoxic T-lymphocyte-associated	1.05	6.19×10^{-1}	-1.18	1.08×10^{-3}

	serine esterase 1)				
ATM	Ataxia telangiectasia mutated	1.04	7.26×10^{-1}	-1.21	7.93×10^{-2}
AKT1	v-akt murine thymoma viral oncogene homolog 1	1.03	6.06×10^{-1}	1.14	1.98×10^{-2}
BOK	BCL2-related ovarian killer	1.01	8.26×10^{-1}	1.11	6.98×10^{-2}
BID	BH3 interacting domain death agonist	1.01	8.65×10^{-1}	1.05	2.70×10^{-1}
BCL2L2	BCL2-like 2	1.01	9.44×10^{-1}	-1.12	1.09×10^{-1}
BMF	Bcl2 modifying factor	-1.00	9.97×10^{-1}	1.12	3.21×10^{-2}
BCL2L1	BCL2-like 1	-1.01	8.91×10^{-1}	-1.02	8.72×10^{-1}
BCL2	B-cell CLL/lymphoma 2	-1.04	4.97×10^{-1}	1.08	8.44×10^{-2}
CASP7	Caspase 7, apoptosis-related cysteine peptidase	-1.04	4.80×10^{-1}	1.02	7.05×10^{-1}
BBC3	BCL2 binding component 3	-1.05	3.36×10^{-1}	1.12	8.96×10^{-3}
DFFB	DNA fragmentation factor, 40 kDa, beta polypeptide (caspase-activated DNase)	-1.05	2.89×10^{-1}	1.03	6.72×10^{-1}
APAF1	Apoptotic peptidase activating factor 1	-1.05	2.49×10^{-1}	-1.04	3.48×10^{-1}
BCL2L10	BCL2-like 10 (apoptosis facilitator)	-1.06	2.93×10^{-1}	1.10	1.04×10^{-1}
CASP9	Caspase 9, apoptosis-related cysteine peptidase	-1.08	1.61×10^{-1}	1.04	4.76×10^{-1}
BIRC2	Baculoviral IAP repeat-containing 2	-1.11	1.48×10^{-1}	-1.30	6.32×10^{-3}
CASP10	Caspase 10, apoptosis-related cysteine peptidase	-1.12	1.46×10^{-1}	1.01	8.79×10^{-1}
BCL2A1	BCL2-related protein A1	-1.12	3.60×10^{-1}	-1.20	5.64×10^{-2}
CASP4	Caspase 4, apoptosis-related cysteine peptidase	-1.13	2.69×10^{-1}	-1.13	2.76×10^{-1}
BAD	BCL2-associated agonist of cell death	-1.14	2.46×10^{-2}	1.06	1.96×10^{-1}
CASP8	Caspase 8, apoptosis-related cysteine peptidase	-1.16	3.38×10^{-2}	-1.20	1.48×10^{-2}

<i>NAIP</i>	NLR family, apoptosis inhibitory protein	-1.23	2.90×10^{-2}	-1.17	6.10×10^{-2}
<i>BIRC3</i>	Baculoviral IAP repeat-containing 3	-1.27	1.25×10^{-1}	1.04	7.99×10^{-1}
<i>CAPN2</i>	Calpain 2, (m/II) large subunit	-1.41	2.71×10^{-4}	-1.22	1.81×10^{-1}
<i>MCL1</i>	Myeloid cell leukemia sequence 1 (BCL2-related)	-1.81	6.44×10^{-8}	-1.59	8.64×10^{-5}
<i>CFLAR</i>	CASP8 and FADD-like apoptosis regulator	-2.34	2.59×10^{-10}	-1.80	1.80×10^{-4}

Table S4. Differential changes in oncogenes

Name	Description	SCC		ADC	
		fold-change	p-value	fold-change	p-value
<i>ECT2</i>	Epithelial cell transforming sequence 2 oncogene	3.59	2.55×10^{-8}	1.54	4.55×10^{-3}
<i>DCUN1D1</i>	DCN1, defective in cullin neddylation 1, domain containing 1 (<i>S. cerevisiae</i>)	2.66	4.00×10^{-7}	-1.06	4.63×10^{-1}
<i>RAB10</i>	RAB10, member RAS oncogene family	1.84	2.24×10^{-5}	1.13	4.28×10^{-1}
<i>RAB25</i>	RAB25, member RAS oncogene family	1.65	2.09×10^{-4}	1.78	1.55×10^{-7}
<i>MET</i>	met proto-oncogene (hepatocyte growth factor receptor)	1.60	8.63×10^{-3}	1.51	3.08×10^{-2}
<i>NAE1</i>	NEDD8 activating enzyme E1 subunit 1	1.59	1.64×10^{-3}	1.10	3.85×10^{-1}
<i>RAP2B</i>	RAP2B, member of RAS oncogene family	1.56	9.39×10^{-5}	1.14	1.07×10^{-2}
<i>MCM3</i>	Minichromosome maintenance complex component 3	1.56	4.24×10^{-5}	1.20	3.48×10^{-2}
<i>SLC4A1AP</i>	Solute carrier family 4 (anion exchanger), member 1, adaptor protein	1.52	4.59×10^{-3}	1.05	7.03×10^{-1}
<i>DEK</i>	DEK oncogene	1.50	2.98×10^{-3}	-1.04	7.59×10^{-1}
<i>RAB38</i>	RAB38, member RAS oncogene family	1.49	4.24×10^{-4}	1.16	3.15×10^{-2}
<i>HRASLS</i>	HRAS-like suppressor	1.48	3.54×10^{-5}	1.36	1.94×10^{-4}
<i>SET</i>	SET nuclear oncogene	1.45	3.91×10^{-5}	1.06	5.01×10^{-1}
<i>KRAS</i>	v-Ki-ras2 Kirsten rat sarcoma viral oncogene homolog	1.45	1.11×10^{-3}	1.01	9.30×10^{-1}
<i>NET1</i>	Neuroepithelial cell transforming 1	1.42	2.25×10^{-4}	1.38	4.58×10^{-5}
<i>P4HB</i>	Prolyl 4-hydroxylase, beta polypeptide	1.42	5.22×10^{-5}	1.45	1.69×10^{-3}
<i>EIF3E</i>	Eukaryotic translation initiation factor 3, subunit E	1.41	6.90×10^{-3}	1.13	3.06×10^{-1}

<i>PARK7</i>	Parkinson disease (autosomal recessive, early onset) 7	1.40	4.04×10^{-4}	1.31	9.36×10^{-3}
<i>TFG</i>	TRK-fused gene	1.39	1.12×10^{-2}	1.21	3.35×10^{-2}
<i>MYBL2</i>	v-myb myeloblastosis viral oncogene homolog (avian)-like 2	1.38	4.82×10^{-7}	1.21	2.09×10^{-3}
<i>MYC</i>	v-myc myelocytomatosis viral oncogene homolog (avian)	1.36	5.01×10^{-2}	-1.21	4.14×10^{-2}
<i>CRKL</i>	v-crk sarcoma virus CT10 oncogene homolog (avian)-like	1.36	8.49×10^{-6}	1.10	1.41×10^{-1}
<i>CTTN</i>	Cortactin	1.35	1.90×10^{-2}	1.22	8.26×10^{-2}
<i>GNB2L1</i>	Guanine nucleotide binding protein (G protein), beta polypeptide 2-like 1	1.32	6.89×10^{-3}	1.04	7.48×10^{-1}
<i>LCN2</i>	Lipocalin 2	1.31	2.80×10^{-2}	-1.00	9.66×10^{-1}
<i>RAN</i>	RAN, member RAS oncogene family	1.31	3.58×10^{-6}	1.28	3.71×10^{-6}
<i>RAB18</i>	RAB18, member RAS oncogene family	1.30	8.31×10^{-2}	-1.13	3.36×10^{-1}
<i>BMI1</i>	BMI1 polycomb ring finger oncogene	1.29	1.26×10^{-2}	1.03	8.21×10^{-1}
<i>RAB30</i>	RAB30, member RAS oncogene family	1.28	8.22×10^{-3}	1.12	1.69×10^{-1}
<i>RAB11A</i>	RAB11A, member RAS oncogene family	1.28	8.28×10^{-2}	-1.41	7.79×10^{-3}
<i>RAB13</i>	RAB13, member RAS oncogene family	1.26	3.18×10^{-2}	1.19	2.55×10^{-1}
<i>RAB6B</i>	RAB6B, member RAS oncogene family	1.26	5.74×10^{-3}	1.11	1.84×10^{-3}
<i>YES1</i>	v-yes-1 Yamaguchi sarcoma viral oncogene homolog 1	1.25	3.59×10^{-2}	-1.04	6.83×10^{-1}
<i>PIM2</i>	pim-2 oncogene	1.24	5.84×10^{-3}	1.23	1.27×10^{-3}
<i>ARHGEF5</i>	Rho guanine nucleotide exchange factor (GEF) 5	1.24	1.80×10^{-2}	1.05	4.13×10^{-1}
<i>MYB</i>	v-myb myeloblastosis viral oncogene homolog (avian)	1.24	4.77×10^{-2}	-1.01	9.21×10^{-1}
<i>HRAS</i>	v-Ha-ras Harvey rat sarcoma viral oncogene homolog	1.23	1.95×10^{-5}	1.19	6.43×10^{-5}

<i>RAB15</i>	RAB15, member RAS oncogene family	1.23	4.39×10^{-3}	1.13	4.13×10^{-2}
<i>EGFR</i>	Epidermal growth factor receptor (erythroblastic leukemia viral (v-erb-b) oncogene homolog, avian)	1.22	1.90×10^{-2}	1.30	1.06×10^{-1}
<i>RAB22A</i>	RAB22A, member RAS oncogene family	1.21	8.18×10^{-3}	1.17	4.41×10^{-2}
<i>TPR</i>	Translocated promoter region (to activated MET oncogene)	1.19	1.23×10^{-1}	-1.04	7.82×10^{-1}
<i>NRAS</i>	Neuroblastoma RAS viral (v-ras) oncogene homolog	1.19	4.03×10^{-2}	1.11	1.30×10^{-1}
<i>RAB9A</i>	RAB9A, member RAS oncogene family	1.18	7.47×10^{-2}	1.03	7.55×10^{-1}
<i>FGFR1OP</i>	FGFR1 oncogene partner	1.18	2.39×10^{-3}	1.01	8.26×10^{-1}
<i>NUP214</i>	Nucleoporin 214 kDa	1.18	3.40×10^{-2}	-1.19	2.16×10^{-2}
<i>RALA</i>	v-ral simian leukemia viral oncogene homolog A (ras related)	1.17	5.29×10^{-2}	1.02	8.17×10^{-1}
<i>FGFR1OP2</i>	FGFR1 oncogene partner 2	1.17	1.84×10^{-1}	1.04	7.76×10^{-1}
<i>EWSR1</i>	Ewing sarcoma breakpoint region 1	1.17	4.91×10^{-2}	-1.09	2.18×10^{-1}
<i>RAB1A</i>	RAB1A, member RAS oncogene family	1.17	2.81×10^{-1}	1.07	6.85×10^{-1}
<i>MAFB</i>	v-maf musculoaponeurotic fibrosarcoma oncogene homolog B (avian)	1.16	9.99×10^{-2}	1.04	5.73×10^{-1}
<i>RUNX1</i>	runt-related transcription factor 1	1.16	3.46×10^{-2}	1.23	3.37×10^{-4}
<i>RAB2A</i>	RAB2A, member RAS oncogene family	1.16	1.31×10^{-1}	1.13	2.68×10^{-1}
<i>FUS</i>	Fusion (involved in t(12;16) in malignant liposarcoma)	1.16	1.21×10^{-1}	-1.02	8.58×10^{-1}
<i>RAB3B</i>	RAB3B, member RAS oncogene family	1.15	9.92×10^{-2}	1.19	3.84×10^{-2}
<i>AKT2</i>	v-akt murine thymoma viral oncogene homolog 2	1.14	9.05×10^{-3}	1.01	8.07×10^{-1}
<i>RAB27B</i>	RAB27B, member RAS oncogene family	1.14	1.22×10^{-1}	1.10	2.80×10^{-1}

<i>HKR1</i>	GLI-Kruppel family member HKR1	1.14	5.99×10^{-2}	1.11	1.08×10^{-2}
<i>ITPA</i>	Inosine triphosphatase (nucleoside triphosphate pyrophosphatase)	1.13	2.09×10^{-2}	1.09	6.25×10^{-2}
<i>MYCL1</i>	v-myc myelocytomatosis viral oncogene homolog 1, lung carcinoma derived (avian)	1.13	1.19×10^{-2}	1.18	1.35×10^{-2}
<i>MERTK</i>	c-mer proto-oncogene tyrosine kinase	1.13	2.82×10^{-1}	1.03	7.69×10^{-1}
<i>BRI3BP</i>	BRI3 binding protein	1.13	5.26×10^{-2}	1.23	4.03×10^{-4}
<i>ENTPD5</i>	ectonucleoside triphosphate diphosphohydrolase 5	1.13	1.89×10^{-1}	1.11	1.60×10^{-1}
<i>RAB1B</i>	RAB1B, member RAS oncogene family	1.12	2.26×10^{-1}	1.07	5.58×10^{-1}
<i>SKIL</i>	SKI-like oncogene	1.12	3.14×10^{-1}	-1.05	6.63×10^{-1}
<i>RAB7A</i>	RAB7A, member RAS oncogene family	1.12	2.95×10^{-1}	-1.27	1.11×10^{-1}
<i>RAB40C</i>	RAB40C, member RAS oncogene family	1.11	8.23×10^{-2}	1.32	1.24×10^{-4}
<i>RAB12</i>	RAB12, member RAS oncogene family	1.11	4.32×10^{-2}	-1.03	5.35×10^{-1}
<i>IRF4</i>	Interferon regulatory factor 4	1.11	1.93×10^{-1}	1.10	2.44×10^{-2}
<i>ELK1</i>	ELK1, member of ETS oncogene family	1.10	4.22×10^{-2}	1.15	6.63×10^{-3}
<i>ETV6</i>	ets variant 6	1.10	3.89×10^{-1}	1.14	7.57×10^{-2}
<i>RAB40B</i>	RAB40B, member RAS oncogene family	1.10	5.42×10^{-2}	1.15	1.38×10^{-3}
<i>TET1</i>	tet oncogene 1	1.10	2.30×10^{-1}	1.03	5.79×10^{-1}
<i>RAB8A</i>	RAB8A, member RAS oncogene family	1.08	4.70×10^{-1}	-1.26	1.09×10^{-1}
<i>RABL4</i>	RAB, member of RAS oncogene family-like 4	1.08	2.30×10^{-1}	1.12	8.22×10^{-2}
<i>BLOC1S2</i>	Biogenesis of lysosomal organelles complex-1, subunit 2	1.08	3.59×10^{-1}	1.01	8.43×10^{-1}
<i>RAB3D</i>	RAB3D, member RAS oncogene family	1.08	1.95×10^{-1}	1.08	2.11×10^{-1}

<i>VAV2</i>	vav 2 guanine nucleotide exchange factor	1.08	3.26×10^{-1}	1.01	8.41×10^{-1}
<i>RAB7L1</i>	RAB7, member RAS oncogene family-like 1	1.07	1.27×10^{-1}	-1.08	1.81×10^{-1}
<i>MRPS11</i>	Mitochondrial ribosomal protein S11	1.07	1.84×10^{-1}	1.17	5.48×10^{-3}
<i>CBL</i>	Cas-Br-M (murine) ecotropic retroviral transforming sequence	1.07	1.83×10^{-1}	-1.03	5.84×10^{-1}
<i>RAP2C</i>	RAP2C, member of RAS oncogene family	1.07	2.09×10^{-1}	1.15	8.69×10^{-4}
<i>RAB6A</i>	RAB6A, member RAS oncogene family	1.07	4.65×10^{-1}	1.01	8.62×10^{-1}
<i>RAB23</i>	RAB23, member RAS oncogene family	1.07	5.96×10^{-1}	-1.32	2.63×10^{-2}
<i>RAB3A</i>	RAB3A, member RAS oncogene family	1.06	1.36×10^{-1}	1.10	7.76×10^{-2}
<i>RAB21</i>	RAB21, member RAS oncogene family	1.06	6.12×10^{-1}	-1.23	1.99×10^{-1}
<i>TMEM50A</i>	Transmembrane protein 50A	1.06	6.51×10^{-1}	-1.06	5.98×10^{-1}
<i>RELB</i>	v-rel reticuloendotheliosis viral oncogene homolog B	1.05	3.13×10^{-1}	1.12	6.33×10^{-2}
<i>RAB26</i>	RAB26, member RAS oncogene family	1.05	3.25×10^{-1}	1.21	1.53×10^{-3}
<i>GLI3</i>	GLI family zinc finger 3	1.05	5.64×10^{-1}	-1.03	6.47×10^{-1}
<i>GLI4</i>	GLI family zinc finger 4	1.04	4.00×10^{-1}	1.14	5.81×10^{-4}
<i>RRAS2</i>	Related RAS viral (r-ras) oncogene homolog 2	1.04	4.13×10^{-1}	1.20	1.64×10^{-4}
<i>NR2F6</i>	Nuclear receptor subfamily 2, group F, member 6	1.04	4.42×10^{-1}	1.23	4.71×10^{-5}
<i>FGF3</i>	Fibroblast growth factor 3 (murine mammary tumor virus integration site (v-int-2) oncogene homolog)	1.04	4.62×10^{-1}	1.21	1.62×10^{-2}
<i>PIM1</i>	pim-1 oncogene	1.04	6.53×10^{-1}	1.07	1.13×10^{-1}
<i>ZSCAN22</i>	Zinc finger and SCAN domain containing 22	1.03	5.80×10^{-1}	1.06	2.53×10^{-1}
<i>DDX6</i>	DEAD (Asp-Glu-Ala-Asp) box polypeptide 6	1.03	8.35×10^{-1}	-1.18	2.93×10^{-1}

<i>RAB35</i>	RAB35, member RAS oncogene family	1.03	7.65×10^{-1}	-1.09	3.27×10^{-1}
<i>ELK4</i>	ELK4, ETS-domain protein (SRF accessory protein 1)	1.03	5.53×10^{-1}	-1.09	8.34×10^{-2}
<i>AKT1</i>	v-akt murine thymoma viral oncogene homolog 1	1.03	6.06×10^{-1}	1.14	1.98×10^{-2}
<i>RAB28</i>	RAB28, member RAS oncogene family	1.03	7.67×10^{-1}	-1.13	3.06×10^{-1}
<i>ERBB3</i>	v-erb-b2 erythroblastic leukemia viral oncogene homolog 3 (avian)	1.03	6.41×10^{-1}	1.22	2.29×10^{-4}
<i>ARAF</i>	v-raf murine sarcoma 3611 viral oncogene homolog	1.03	6.08×10^{-1}	1.10	2.20×10^{-2}
<i>ETV7</i>	ets variant 7	1.03	6.19×10^{-1}	-1.01	8.07×10^{-1}
<i>RAB34</i>	RAB34, member RAS oncogene family	1.03	5.98×10^{-1}	1.24	1.77×10^{-6}
<i>MAFG</i>	v-maf musculoaponeurotic fibrosarcoma oncogene homolog G (avian)	1.02	5.43×10^{-1}	1.04	2.90×10^{-1}
<i>RAB14</i>	RAB14, member RAS oncogene family	1.02	8.66×10^{-1}	-1.57	3.44×10^{-3}
<i>RAB3C</i>	RAB3C, member RAS oncogene family	1.02	7.84×10^{-1}	-1.05	4.08×10^{-1}
<i>MAF</i>	v-maf musculoaponeurotic fibrosarcoma oncogene homolog (avian)	1.02	7.34×10^{-1}	-1.13	2.73×10^{-3}
<i>RAB39B</i>	RAB39B, member RAS oncogene family	1.02	7.28×10^{-1}	-1.02	7.92×10^{-1}
<i>RET</i>	ret proto-oncogene	1.02	6.56×10^{-1}	1.01	8.71×10^{-1}
<i>RALB</i>	v-ral simian leukemia viral oncogene homolog B (ras related; GTP binding protein)	1.02	8.65×10^{-1}	-1.35	8.13×10^{-3}
<i>SRC</i>	v-src sarcoma (Schmidt-Ruppin A-2) viral oncogene homolog (avian)	1.02	6.52×10^{-1}	1.10	2.50×10^{-2}
<i>TTC23</i>	Tetratricopeptide repeat domain 23	1.02	7.68×10^{-1}	-1.03	4.95×10^{-1}
<i>WNT3</i>	Wingless-type MMTV integration site family, member 3	1.02	7.43×10^{-1}	1.20	5.90×10^{-4}
<i>GLI1</i>	GLI family zinc finger 1	1.02	7.63×10^{-1}	1.12	7.94×10^{-2}

<i>GLI2</i>	GLI family zinc finger 2	1.02	7.61×10^{-1}	1.11	3.29×10^{-2}
<i>MAFA</i>	v-maf musculoaponeurotic fibrosarcoma oncogene homolog A (avian)	1.01	8.88×10^{-1}	1.15	8.23×10^{-3}
<i>RHOC</i>	ras homolog gene family, member C	1.01	9.24×10^{-1}	1.08	2.34×10^{-1}
<i>RAB24</i>	RAB24, member RAS oncogene family	1.01	8.90×10^{-1}	1.06	1.48×10^{-1}
<i>RAB33B</i>	RAB33B, member RAS oncogene family	1.01	9.39×10^{-1}	1.11	1.03×10^{-1}
<i>EPHA1</i>	EPH receptor A1	1.00	8.99×10^{-1}	1.08	7.17×10^{-2}
<i>RAB5B</i>	RAB5B, member RAS oncogene family	1.00	9.91×10^{-1}	-1.11	3.12×10^{-1}
<i>WNT1</i>	Wingless-type MMTV integration site family, member 1	1.00	9.91×10^{-1}	1.13	2.91×10^{-2}
<i>CRK</i>	v-crk sarcoma virus CT10 oncogene homolog (avian)	-1.00	9.49×10^{-1}	1.06	3.64×10^{-1}
<i>TCL1A</i>	T-cell leukemia/lymphoma 1A	-1.00	9.51×10^{-1}	1.12	5.70×10^{-2}
<i>RABL5</i>	RAB, member RAS oncogene family-like 5	-1.01	9.11×10^{-1}	1.05	3.03×10^{-1}
<i>RAB33A</i>	RAB33A, member RAS oncogene family	-1.01	8.79×10^{-1}	1.08	2.20×10^{-1}
<i>RAB5C</i>	RAB5C, member RAS oncogene family	-1.01	9.07×10^{-1}	1.07	4.51×10^{-1}
<i>MCF2</i>	MCF.2 cell line derived transforming sequence	-1.01	8.35×10^{-1}	1.13	2.25×10^{-2}
<i>MYCN</i>	v-myc myelocytomatosis viral related oncogene, neuroblastoma derived (avian)	-1.01	8.23×10^{-1}	1.16	1.08×10^{-2}
<i>ABL2</i>	v-abl Abelson murine leukemia viral oncogene homolog 2 (arg, Abelson-related gene)	-1.01	8.34×10^{-1}	1.09	5.15×10^{-2}
<i>FGF4</i>	Fibroblast growth factor 4	-1.01	7.91×10^{-1}	1.13	1.70×10^{-2}
<i>SSPN</i>	Sarcospan (Kras oncogene-associated gene)	-1.01	8.01×10^{-1}	1.00	9.41×10^{-1}
<i>MOS</i>	v-mos Moloney murine sarcoma viral oncogene homolog	-1.02	8.30×10^{-1}	1.03	6.99×10^{-1}

<i>RAB11B</i>	RAB11B, member RAS oncogene family	-1.02	8.33×10^{-1}	-1.04	4.85×10^{-1}
<i>RAB2B</i>	RAB2B, member RAS oncogene family	-1.02	8.57×10^{-1}	-1.17	9.91×10^{-2}
<i>ERAS</i>	ES cell expressed Ras	-1.02	7.42×10^{-1}	1.13	1.49×10^{-2}
<i>RGL2</i>	ral guanine nucleotide dissociation stimulator-like 2	-1.02	7.53×10^{-1}	1.00	9.86×10^{-1}
<i>RAB4B</i>	RAB4B, member RAS oncogene family	-1.02	6.15×10^{-1}	1.06	2.23×10^{-1}
<i>RABL3</i>	RAB, member of RAS oncogene family-like 3	-1.02	8.66×10^{-1}	1.04	7.08×10^{-1}
<i>RAB7B</i>	RAB7B, member RAS oncogene family	-1.02	5.44×10^{-1}	1.02	5.34×10^{-1}
<i>LCK</i>	Lymphocyte-specific protein tyrosine kinase	-1.03	6.40×10^{-1}	1.06	2.08×10^{-1}
<i>FEV</i>	FEV (ETS oncogene family)	-1.03	6.62×10^{-1}	1.18	5.08×10^{-3}
<i>RAB5A</i>	RAB5A, member RAS oncogene family	-1.03	7.21×10^{-1}	-1.04	7.41×10^{-1}
<i>NTRK1</i>	Neurotrophic tyrosine kinase, receptor, type 1	-1.03	5.13×10^{-1}	1.09	7.97×10^{-2}
<i>MMEL1</i>	Membrane metallo-endopeptidase-like 1	-1.03	5.53×10^{-1}	1.07	1.92×10^{-1}
<i>THPO</i>	Thrombopoietin	-1.03	5.85×10^{-1}	1.04	4.43×10^{-1}
<i>CALCA</i>	Calcitonin-related polypeptide alpha	-1.03	5.76×10^{-1}	1.25	2.73×10^{-1}
<i>BCL2</i>	B-cell CLL/lymphoma 2	-1.04	4.97×10^{-1}	1.08	8.44×10^{-2}
<i>CCND1</i>	cyclin D1	-1.04	6.52×10^{-1}	1.06	4.94×10^{-1}
<i>ELK3</i>	ELK3, ETS-domain protein (SRF accessory protein 2)	-1.04	6.50×10^{-1}	1.00	9.81×10^{-1}
<i>TLX1</i>	T-cell leukemia homeobox 1	-1.04	6.24×10^{-1}	1.05	3.92×10^{-1}
<i>ERBB2</i>	v-erb-b2 erythroblastic leukemia viral oncogene homolog 2, neuro/glioblastoma derived oncogene homolog (avian)	-1.04	5.39×10^{-1}	1.12	1.47×10^{-2}
<i>RELA</i>	v-rel reticuloendotheliosis viral oncogene homolog A (avian)	-1.04	4.91×10^{-1}	-1.01	8.22×10^{-1}

<i>RAB6C</i>	RAB6C, member RAS oncogene family	-1.04	6.76×10^{-1}	-1.25	1.04×10^{-1}
<i>RAB36</i>	RAB36, member RAS oncogene family	-1.05	3.46×10^{-1}	-1.09	7.18×10^{-2}
<i>MAS1L</i>	MAS1 oncogene-like	-1.05	4.83×10^{-1}	1.04	5.47×10^{-1}
<i>RAB32</i>	RAB32, member RAS oncogene family	-1.05	3.54×10^{-1}	1.11	5.44×10^{-2}
<i>RAB39</i>	RAB39, member RAS oncogene family	-1.05	4.87×10^{-1}	1.04	5.47×10^{-1}
<i>MPL</i>	Myeloproliferative leukemia virus oncogene	-1.06	1.56×10^{-1}	-1.02	5.97×10^{-1}
<i>RAB43</i>	RAB43, member RAS oncogene family	-1.06	4.88×10^{-1}	-1.00	9.83×10^{-1}
<i>RAB40AL</i>	RAB40A, member RAS oncogene family-like	-1.07	4.55×10^{-1}	1.02	7.75×10^{-1}
<i>RAP2A</i>	RAP2A, member of RAS oncogene family	-1.07	4.17×10^{-1}	-1.00	9.80×10^{-1}
<i>FOXG1</i>	Forkhead box G1	-1.07	1.79×10^{-1}	1.16	1.04×10^{-2}
<i>RAB9B</i>	RAB9B, member RAS oncogene family	-1.08	1.73×10^{-1}	-1.02	7.98×10^{-1}
<i>TCL1B</i>	T-cell leukemia/lymphoma 1B	-1.08	1.63×10^{-1}	1.11	1.35×10^{-1}
<i>RAB41</i>	RAB41, member RAS oncogene family	-1.08	1.18×10^{-1}	1.02	8.04×10^{-1}
<i>MAFK</i>	v-maf musculoaponeurotic fibrosarcoma oncogene homolog K (avian)	-1.09	2.72×10^{-1}	1.01	8.87×10^{-1}
<i>BRAF</i>	v-raf murine sarcoma viral oncogene homolog B1	-1.09	2.94×10^{-1}	-1.08	4.62×10^{-1}
<i>PIM3</i>	pim-3 oncogene	-1.09	1.28×10^{-1}	-1.02	6.60×10^{-1}
<i>WNT7A</i>	Wingless-type MMTV integration site family, member 7A	-1.10	1.56×10^{-1}	-1.01	7.82×10^{-1}
<i>REL</i>	v-rel reticuloendotheliosis viral oncogene homolog (avian)	-1.10	3.90×10^{-1}	-1.01	9.05×10^{-1}
<i>CDON</i>	Cdon homolog (mouse)	-1.10	9.39×10^{-2}	-1.10	1.27×10^{-1}
<i>RAB20</i>	RAB20, member RAS oncogene family	-1.10	1.83×10^{-1}	1.03	5.64×10^{-1}

<i>MRAS</i>	Muscle RAS oncogene homolog	-1.11	3.69×10^{-1}	-1.03	5.95×10^{-1}
<i>CSF1R</i>	Colony stimulating factor 1 receptor	-1.11	9.25×10^{-2}	1.02	6.44×10^{-1}
<i>RAF1</i>	v-raf-1 murine leukemia viral oncogene homolog 1	-1.11	1.74×10^{-1}	-1.21	8.95×10^{-3}
<i>ADRB1</i>	Adrenergic, beta-1-, receptor	-1.11	9.67×10^{-2}	1.08	2.08×10^{-1}
<i>SKI</i>	v-ski sarcoma viral oncogene homolog (avian)	-1.11	3.55×10^{-2}	1.08	7.68×10^{-2}
<i>THRB</i>	Thyroid hormone receptor, beta (erythroblastic leukemia viral (v-erb-a) oncogene homolog 2, avian)	-1.12	4.74×10^{-2}	-1.12	3.33×10^{-2}
<i>FRAT1</i>	Frequently rearranged in advanced T-cell lymphomas	-1.12	5.73×10^{-2}	1.01	8.37×10^{-1}
<i>VAV1</i>	vav 1 guanine nucleotide exchange factor	-1.13	3.25×10^{-2}	-1.00	9.95×10^{-1}
<i>RAP1B</i>	RAP1B, member of RAS oncogene family	-1.14	4.41×10^{-1}	-1.73	5.82×10^{-3}
<i>RAB37</i>	RAB37, member RAS oncogene family	-1.14	1.23×10^{-2}	1.08	2.00×10^{-1}
<i>EEF1A1</i>	Eukaryotic translation elongation factor 1 alpha 1	-1.14	2.38×10^{-1}	-1.16	8.13×10^{-2}
<i>RAB42</i>	RAB42, member RAS oncogene family	-1.14	1.74×10^{-1}	-1.01	8.90×10^{-1}
<i>ABL1</i>	c-abl oncogene 1, receptor tyrosine kinase	-1.14	1.85×10^{-2}	-1.08	2.07×10^{-1}
<i>RABL2B</i>	RAB, member of RAS oncogene family-like 2B	-1.15	1.66×10^{-2}	-1.20	4.97×10^{-3}
<i>MAS1</i>	MAS1 oncogene	-1.15	3.62×10^{-2}	1.02	8.03×10^{-1}
<i>FES</i>	Feline sarcoma oncogene	-1.16	6.14×10^{-3}	-1.05	2.91×10^{-1}
<i>EVI1</i>	Ecotropic viral integration site 1	-1.16	6.96×10^{-2}	-1.00	9.99×10^{-1}
<i>RAPGEF1</i>	Rap guanine nucleotide exchange factor (GEF) 1	-1.17	3.54×10^{-2}	-1.15	2.36×10^{-2}
<i>PEA15</i>	Phosphoprotein enriched in astrocytes 15	-1.18	1.23×10^{-1}	-1.26	5.63×10^{-2}
<i>CXCL1</i>	Chemokine (C-X-C motif) ligand 1 (melanoma growth stimulating	-1.18	2.07×10^{-1}	1.14	2.77×10^{-1}

	activity, alpha)				
<i>RAB40A</i>	RAB40A, member RAS oncogene family	-1.19	2.68×10^{-3}	-1.05	3.04×10^{-1}
<i>RAB31</i>	RAB31, member RAS oncogene family	-1.20	1.56×10^{-1}	-1.09	4.61×10^{-1}
<i>PDGFB</i>	Platelet-derived growth factor beta polypeptide (simian sarcoma viral (v-sis) oncogene homolog)	-1.20	2.55×10^{-3}	-1.06	3.65×10^{-1}
<i>RAP1A</i>	RAP1A, member of RAS oncogene family	-1.21	6.05×10^{-2}	-1.27	1.90×10^{-2}
<i>ERBB4</i>	v-erb-a erythroblastic leukemia viral oncogene homolog 4 (avian)	-1.21	1.81×10^{-3}	-1.01	9.02×10^{-1}
<i>USP6</i>	Ubiquitin specific peptidase 6 (Tre-2 oncogene)	-1.22	9.09×10^{-3}	-1.10	1.22×10^{-1}
<i>RABL2A</i>	RAB, member of RAS oncogene family-like 2A	-1.22	7.63×10^{-3}	-1.24	7.50×10^{-3}
<i>RRAS</i>	Related RAS viral (r-ras) oncogene homolog	-1.23	3.91×10^{-3}	-1.09	1.81×10^{-1}
<i>VAV3</i>	vav 3 guanine nucleotide exchange factor	-1.23	1.18×10^{-2}	-1.27	7.05×10^{-3}
<i>SPAG9</i>	Sperm associated antigen 9	-1.24	5.45×10^{-2}	-1.31	5.09×10^{-2}
<i>RHOA</i>	ras homolog gene family, member A	-1.24	3.95×10^{-3}	-1.29	4.22×10^{-3}
<i>RASEF</i>	RAS and EF-hand domain containing	-1.25	3.74×10^{-3}	1.07	4.46×10^{-1}
<i>THRA</i>	Thyroid hormone receptor, alpha (erythroblastic leukemia viral (v-erb-a) oncogene homolog, avian)	-1.26	6.05×10^{-3}	-1.19	2.69×10^{-2}
<i>MYBL1</i>	v-myb myeloblastosis viral oncogene homolog (avian)-like 1	-1.26	1.63×10^{-2}	-1.09	2.27×10^{-1}
<i>AXL</i>	AXL receptor tyrosine kinase	-1.26	7.17×10^{-6}	-1.12	2.65×10^{-2}
<i>RBM6</i>	RNA binding motif protein 6	-1.27	4.86×10^{-2}	-1.29	7.04×10^{-2}
<i>USP4</i>	Ubiquitin specific peptidase 4 (proto-oncogene)	-1.28	2.69×10^{-3}	-1.39	9.25×10^{-4}
<i>RAB17</i>	RAB17, member RAS oncogene family	-1.30	1.70×10^{-4}	1.02	6.96×10^{-1}

<i>FGR</i>	Gardner-Rasheed feline sarcoma viral (v-fgr) oncogene homolog	-1.31	1.67×10^{-4}	-1.08	8.29×10^{-2}
<i>CXCL3</i>	Chemokine (C-X-C motif) ligand 3	-1.32	7.93×10^{-4}	1.11	8.52×10^{-2}
<i>LYN</i>	v-yes-1 Yamaguchi sarcoma viral related oncogene homolog	-1.34	1.16×10^{-2}	1.02	8.30×10^{-1}
<i>NR2F1</i>	Nuclear receptor subfamily 2, group F, member 1	-1.36	2.47×10^{-6}	-1.10	6.90×10^{-2}
<i>MAP3K8</i>	Mitogen-activated protein kinase kinase kinase 8	-1.36	7.46×10^{-5}	-1.22	9.21×10^{-3}
<i>FYN</i>	FYN oncogene related to SRC, FGR, YES	-1.38	6.05×10^{-4}	-1.62	3.58×10^{-5}
<i>MAFF</i>	v-maf musculoaponeurotic fibrosarcoma oncogene homolog F (avian)	-1.40	5.49×10^{-4}	-1.03	6.47×10^{-1}
<i>RAB27A</i>	RAB27A, member RAS oncogene family	-1.42	6.41×10^{-4}	-1.12	3.27×10^{-1}
<i>ARHGEF12</i>	Rho guanine nucleotide exchange factor (GEF) 12	-1.43	6.51×10^{-3}	-1.48	3.45×10^{-2}
<i>JUND</i>	jun D proto-oncogene	-1.44	1.75×10^{-8}	-1.13	5.28×10^{-3}
<i>RHOB</i>	ras homolog gene family, member B	-1.45	1.96×10^{-7}	-1.08	2.13×10^{-1}
<i>ETS2</i>	v-ets erythroblastosis virus E26 oncogene homolog 2 (avian)	-1.58	6.93×10^{-6}	-1.43	1.35×10^{-2}
<i>JUNB</i>	jun B proto-oncogene	-1.60	9.51×10^{-4}	-1.35	2.70×10^{-2}
<i>FER</i>	fer (fps/fes related) tyrosine kinase	-1.61	1.72×10^{-4}	-1.52	1.50×10^{-3}
<i>ETS1</i>	v-ets erythroblastosis virus E26 oncogene homolog 1 (avian)	-1.67	1.63×10^{-4}	-1.63	1.55×10^{-4}
<i>FLI1</i>	Friend leukemia virus integration 1	-1.68	1.69×10^{-8}	-1.63	7.05×10^{-6}
<i>ERG</i>	v-ets erythroblastosis virus E26 oncogene homolog (avian)	-1.72	4.38×10^{-8}	-1.36	2.34×10^{-3}
<i>RAB8B</i>	RAB8B, member RAS oncogene family	-1.76	1.24×10^{-3}	-1.92	3.62×10^{-4}
<i>KIT</i>	v-kit Hardy-Zuckerman 4 feline sarcoma viral oncogene homolog	-1.84	2.08×10^{-4}	-1.34	4.29×10^{-2}
<i>AKAP13</i>	A kinase (PRKA) anchor protein	-1.87	3.77×10^{-10}	-1.57	1.75×10^{-4}

	13				
<i>AKT3</i>	v-akt murine thymoma viral oncogene homolog 3 (protein kinase B, gamma)	-1.88	4.68×10^{-4}	-1.83	2.81×10^{-4}
<i>KLF6</i>	Kruppel-like factor 6	-1.97	6.09×10^{-9}	-1.46	2.99×10^{-4}
<i>JUN</i>	jun oncogene	-2.30	7.39×10^{-9}	-1.72	1.19×10^{-4}
<i>FOS</i>	v-fos FBJ murine osteosarcoma viral oncogene homolog	-2.80	7.18×10^{-7}	-2.02	9.18×10^{-4}
<i>ROS1</i>	c-ros oncogene 1 , receptor tyrosine kinase	-2.97	8.79×10^{-9}	-1.22	3.44×10^{-1}
<i>CXCL2</i>	Chemokine (C-X-C motif) ligand 2	-3.65	2.45×10^{-8}	-1.69	4.68×10^{-4}
<i>FOSB</i>	FBJ murine osteosarcoma viral oncogene homolog B	-4.65	1.60×10^{-9}	-2.14	4.87×10^{-4}

Table S5. Differential changes in tumor suppressors

Name	Description	SCC		ADC	
		fold-change	p-value	fold-change	p-value
<i>DLG1</i>	Discs, large homolog 1 (<i>Drosophila</i>)	2.41	3.46×10^{-5}	-1.15	3.72×10^{-1}
<i>DLGAP5</i>	Discs, large (<i>Drosophila</i>) homolog-associated protein 5	2.35	4.22×10^{-7}	1.42	1.13×10^{-4}
<i>FAT</i>	FAT tumor suppressor homolog 1 (<i>Drosophila</i>)	1.95	1.64×10^{-5}	1.34	2.29×10^{-2}
<i>TRIM59</i>	Tripartite motif-containing 59	1.55	8.23×10^{-5}	1.21	4.97×10^{-6}
<i>FAT2</i>	FAT tumor suppressor homolog 2 (<i>Drosophila</i>)	1.52	3.83×10^{-5}	1.10	6.39×10^{-2}
<i>SMARCB1</i>	SWI/SNF related, matrix associated, actin dependent regulator of chromatin, subfamily b, member 1	1.48	3.47×10^{-5}	1.10	1.62×10^{-1}
<i>CDKN2A</i>	Cyclin-dependent kinase inhibitor 2A (melanoma, p16, inhibits CDK4)	1.32	2.06×10^{-2}	1.26	1.15×10^{-3}
<i>TUSC3</i>	Tumor suppressor candidate 3	1.29	4.14×10^{-2}	-1.01	9.36×10^{-1}
<i>ING2</i>	Inhibitor of growth family, member 2	1.25	7.19×10^{-2}	1.18	2.65×10^{-1}
<i>ST13</i>	Suppression of tumorigenicity 13 (colon carcinoma) (Hsp70 interacting protein)	1.25	7.53×10^{-2}	-1.10	4.53×10^{-1}
<i>EXT1</i>	Exostoses (multiple) 1	1.19	1.50×10^{-1}	-1.07	3.64×10^{-1}
<i>TP53</i>	Tumor protein p53	1.18	6.27×10^{-2}	1.09	1.88×10^{-1}
<i>VHL</i>	von Hippel-Lindau tumor suppressor	1.17	1.60×10^{-2}	1.20	1.02×10^{-3}
<i>BRCA2</i>	Breast cancer 2, early onset	1.17	1.61×10^{-2}	1.02	6.07×10^{-1}
<i>RB1</i>	Retinoblastoma 1	1.15	1.57×10^{-1}	-1.40	1.93×10^{-3}
<i>LATS1</i>	LATS, large tumor suppressor, homolog 1 (<i>Drosophila</i>)	1.15	3.78×10^{-2}	-1.15	2.59×10^{-2}
<i>POU6F2</i>	POU class 6 homeobox 2	1.14	3.07×10^{-2}	1.10	1.35×10^{-1}
<i>CELSR2</i>	Cadherin, EGF LAG seven-pass G-type receptor 2 (flamingo)	1.12	9.52×10^{-3}	1.10	4.80×10^{-3}

	homolog, <i>Drosophila</i>)				
<i>PDGFRL</i>	Platelet-derived growth factor receptor-like	1.12	1.91×10^{-1}	1.15	1.60×10^{-2}
<i>BAX</i>	BCL2-associated X protein	1.10	5.67×10^{-2}	1.21	4.78×10^{-4}
<i>EXT2</i>	Exostoses (multiple) 2	1.09	1.17×10^{-1}	1.00	9.21×10^{-1}
<i>RARB</i>	Retinoic acid receptor, beta	1.09	2.37×10^{-1}	-1.12	9.82×10^{-2}
<i>ING1</i>	Inhibitor of growth family, member 1	1.08	1.68×10^{-1}	1.10	2.26×10^{-2}
<i>FH</i>	Fumarate hydratase	1.07	3.18×10^{-1}	1.06	4.42×10^{-1}
<i>EAF2</i>	ELL associated factor 2	1.07	3.09×10^{-1}	1.06	2.95×10^{-1}
<i>ING4</i>	Inhibitor of growth family, member 4	1.07	2.85×10^{-1}	-1.01	8.93×10^{-1}
<i>FAM123B</i>	Family with sequence similarity 123B	1.06	2.78×10^{-1}	1.06	2.86×10^{-1}
<i>ST7L</i>	Suppression of tumorigenicity 7 like	1.05	2.52×10^{-1}	-1.04	2.28×10^{-1}
<i>STEAP3</i>	STEAP family member 3	1.05	2.84×10^{-1}	1.15	3.35×10^{-3}
<i>SMAD2</i>	SMAD family member 2	1.04	7.32×10^{-1}	1.04	7.07×10^{-1}
<i>FAM10A4</i>	Family with sequence similarity 10, member A4 pseudogene	1.04	5.94×10^{-1}	1.00	9.97×10^{-1}
<i>CEBPA</i>	CCAAT/enhancer binding protein (C/EBP), alpha	1.02	6.95×10^{-1}	1.30	3.27×10^{-5}
<i>MN1</i>	Meningioma (disrupted in balanced translocation) 1	1.02	7.36×10^{-1}	1.16	7.45×10^{-3}
<i>PTCH1</i>	Patched homolog 1 (<i>Drosophila</i>)	1.01	8.18×10^{-1}	-1.04	3.97×10^{-1}
<i>Pinx1</i>	PIN2-interacting protein 1	1.01	9.32×10^{-1}	1.09	1.86×10^{-1}
<i>TUSC2</i>	Tumor suppressor candidate 2	1.00	9.53×10^{-1}	1.15	4.09×10^{-3}
<i>DLEU1</i>	Deleted in lymphocytic leukemia 1 (non-protein coding)	-1.00	1.00	-1.01	9.22×10^{-1}
<i>LZTS2</i>	Leucine zipper, putative tumor suppressor 2	-1.00	9.07×10^{-1}	1.02	6.23×10^{-1}
<i>GLTSCR1</i>	Glioma tumor suppressor candidate region gene 1	-1.00	9.22×10^{-1}	1.11	4.39×10^{-2}

<i>CDKN1B</i>	Cyclin-dependent kinase inhibitor 1B (p27, Kip1)	-1.01	9.27×10^{-1}	-1.09	3.39×10^{-1}
<i>CDKN2B</i>	Cyclin-dependent kinase inhibitor 2B (p15, inhibits CDK4)	-1.01	8.38×10^{-1}	1.20	3.78×10^{-3}
<i>TUSC4</i>	Tumor suppressor candidate 4	-1.02	6.06×10^{-1}	1.09	3.35×10^{-2}
<i>OVCA2</i>	Candidate tumor suppressor in ovarian cancer 2	-1.03	4.47×10^{-1}	1.06	7.07×10^{-2}
<i>ARL11</i>	ADP-ribosylation factor-like 11	-1.03	5.57×10^{-1}	-1.02	7.04×10^{-1}
<i>TUSC1</i>	Tumor suppressor candidate 1	-1.04	4.24×10^{-1}	1.10	2.77×10^{-2}
<i>RPH3AL</i>	Rabphilin 3A-like (without C2 domains)	-1.05	2.56×10^{-1}	1.23	1.24×10^{-4}
<i>RASSF5</i>	Ras association (RalGDS/AF-6) domain family member 5	-1.05	3.58×10^{-1}	-1.04	5.09×10^{-1}
<i>SMAD4</i>	SMAD family member 4	-1.05	5.53×10^{-1}	-1.25	3.24×10^{-2}
<i>TUSC5</i>	Tumor suppressor candidate 5	-1.06	4.42×10^{-1}	1.06	3.31×10^{-1}
<i>CDK2AP2</i>	Cyclin-dependent kinase 2 associated protein 2	-1.08	2.48×10^{-1}	1.21	4.60×10^{-4}
<i>RASSF4</i>	Ras association (RalGDS/AF-6) domain family member 4	-1.09	3.73×10^{-1}	1.07	1.88×10^{-1}
<i>NKX3-1</i>	NK3 homeobox 1	-1.09	1.07×10^{-1}	1.04	4.59×10^{-1}
<i>LZTS1</i>	Leucine zipper, putative tumor suppressor 1	-1.09	1.90×10^{-1}	1.08	1.94×10^{-1}
<i>APC</i>	Adenomatous polyposis coli	-1.09	3.95×10^{-1}	-1.29	9.09×10^{-4}
<i>PTEN</i>	Phosphatase and tensin homolog	-1.09	3.01×10^{-1}	-1.03	6.85×10^{-1}
<i>CYB561D 2</i>	Cytochrome b-561 domain containing 2	-1.10	1.39×10^{-1}	1.04	5.50×10^{-1}
<i>VHLL</i>	von Hippel-Lindau tumor suppressor-like	-1.13	5.81×10^{-2}	-1.04	5.23×10^{-1}
<i>FLCN</i>	Folliculin	-1.13	2.29×10^{-2}	1.04	3.91×10^{-1}
<i>RASSF1</i>	Ras association (RalGDS/AF-6) domain family member 1	-1.15	4.18×10^{-2}	1.06	1.81×10^{-1}
<i>LATS2</i>	LATS, large tumor suppressor, homolog 2 (<i>Drosophila</i>)	-1.15	2.82×10^{-3}	1.02	5.47×10^{-1}
<i>RPL10</i>	Ribosomal protein L10	-1.17	1.78×10^{-1}	1.05	7.52×10^{-1}

<i>GLTSCR2</i>	Glioma tumor suppressor candidate region gene 2	-1.18	2.94×10^{-3}	-1.13	6.14×10^{-2}
<i>SPI1</i>	Spleen focus forming virus (SFFV) proviral integration oncogene spi1	-1.20	4.56×10^{-3}	1.05	2.56×10^{-1}
<i>HYAL1</i>	Hyaluronoglucosaminidase 1	-1.20	5.25×10^{-4}	-1.10	4.64×10^{-2}
<i>FAT3</i>	FAT tumor suppressor homolog 3 (<i>Drosophila</i>)	-1.20	5.88×10^{-4}	-1.07	2.91×10^{-1}
<i>MTUS1</i>	Mitochondrial tumor suppressor 1	-1.25	4.10×10^{-2}	-1.08	5.09×10^{-1}
<i>DCC</i>	Deleted in colorectal carcinoma	-1.27	1.47×10^{-3}	-1.14	4.26×10^{-2}
<i>FAT4</i>	FAT tumor suppressor homolog 4 (<i>Drosophila</i>)	-1.44	1.87×10^{-7}	-1.43	3.55×10^{-7}
<i>CADM1</i>	Cell adhesion molecule 1	-1.98	1.00×10^{-7}	-1.24	3.08×10^{-2}
<i>TGFBR2</i>	Transforming growth factor, beta receptor II (70/80 kDa)	-2.09	1.85×10^{-11}	-1.81	2.09×10^{-7}